
Article

Modeling and analysis of the operational and investment costs of hydrogen sea transportation applied to NH₃ and LH₂ energy derivatives

Cayet Pierre¹, Gharbi Oualid², and Le Goff Elise³

¹CEA/DES/I-Tésé, Université Paris Saclay, Gif sur Yvette, France

²CEA/DES/I-Tésé, Université Paris Saclay, Gif sur Yvette, France

³Laboratory for Innovation in Technology for Energy and New Materials of the French Alternative Energies and Atomic Energy Commission (CEA/DES/Liten)

January 5, 2026

Abstract

The paper introduces a multi-regional, multi-commodity investment and operational optimization model to evaluate the levelised transportation cost of hydrogen and its derivatives for specific maritime trade routes¹. It is formulated as a Mixed-Integer Linear Programming (MILP) with both annual investment and daily operational decisions, covering conversion, export terminal storage, transportation, import terminal storage and reconversion flows. Our model both accounts for stock and flow constraints, and includes factors influencing transportation costs such as maritime distance, port charges and canal fees, ship size and required power, fuel consumption and boil-off gas (BOG) losses. We keep track of the number of vessels used for shipping using integer variables, with explicit constraints on fuel requirements for ships using their own cargo for propulsion. The model, coupled with a comprehensive cost decomposition, allows us to track non-linearities in the dynamics of cost categories and economies of scale for extremely low to large import volumes of hydrogen and its derivatives. This allows to derive the minimum efficient scale for specific maritime trade routes and provide a precise decomposition of the share of each cost category in the total cost for various trade volumes, in addition to their allocation between exporting and importing regions. The results indicate a consistent transportation cost differential in favour of NH₃ when compared to LH₂, even when accounting for the extra-cost associated to the conversion and reconversion of hydrogen to and from NH₃. We also provide a short econometric analysis of the effects of a subset of exogenous parameters identified in the literature on hydrogen transportation cost. Our results provide a robust and comprehensive quantitative basis for further analysis of investment decisions and coordination issues relative to the early-stages of an international hydrogen supply chain, in particular when risk aversion and cost uncertainties are considered.

Keywords: Hydrogen transport, Ammonia, Liquefied Hydrogen, Levelized shipping cost

¹This work has benefited from funding by the French National Research Agency (ANR) under the project reference ANR-23-CE05-0022 (GET-MORE-H2).

Contents

Introduction	2
1 H2-derivatives Maritime Transport model	8
1.1 Theoretical Formalization	8
1.1.1 Parameters and Variables	8
1.1.2 Objective Function	12
1.1.3 Technical constraints	13
1.1.4 Modeling assumptions	17
1.2 Database and empirical assumptions	18
1.2.1 Routes and distances	18
1.2.2 Geographical coverage	18
1.2.3 Technological and technical parameters	19
1.2.4 Economic parameters	20
2 International hydrogen trade case study	20
2.1 Measuring the strength of economies of scale	20
2.2 Unit cost distribution analysis, by energy carrier and technology size	23
2.3 Cost distribution analysis by cost category	29
2.4 Total cost analysis	38
2.5 Econometric insights of exogenous factors influencing H2 transportation cost	42
3 Conclusions	44
4 Appendix	45

Introduction

Faced with forecasts of high demand over the medium to long term, the production of low-carbon hydrogen derivatives is becoming a major challenge for achieving zero carbon emissions. In 2023, global hydrogen production represented 97Mt and was mainly produced from unabated fossil fuels with natural gas and coal without Carbon Capture Utilisation and Storage (CCUS); about 15% of hydrogen was produced as a by-product in refineries and petrochemical industry (International Energy Agency, 2024a). Low-carbon hydrogen production was less than 1MtH₂ and derived mainly from fossil fuels with CCUS technologies, with production from water electrolysis less than 100 ktH₂. Electrolytic hydrogen production represented only a very small share of the total, with Alkaline technology (ALK) continuing to account for the largest share, followed by Proton Exchange Membrane (PEM) and Solid Oxide Electrolysis Cell (SOEC). The expansion of manufacturing capacity is expected to drive down electrolyser costs as has occurred with solar PV and battery manufacturing in the past. In 2024, investment in hydrogen electrolysers grew by more than 140% to reach 5 billion€ specially to replace existing use of fossil-fuels hydrogen in refining and chemical industry (International Energy Agency, 2024b) even if the cost of water electrolyser increased in recent years due to higher materials and labor costs. In 2023, the capital cost of an installed electrolyser ranged between 2000\$US/kW for alkaline and 2450\$US/kW for PEM electrolysers compared to the natural gas reforming without CCUS with 720\$US/kW (International Energy Agency, 2024a) which slowed the adoption of water electrolysis technology.

In addition to the high investment costs, low-carbon hydrogen production requests additional consumption of electricity which will increase very significantly the demand for electricity and the needs for installed renewable energy capacities. In 2050, the installed capacity of renewable for hydrogen production reaches more 3000 GW and 5000 GW for respectively APS ("Announced Pledges Scenario") and NZE ("Net Zero Emissions") Scenario (International Energy Agency, 2024c) and the almost of this additional capacity comes from solar PV (80% for the NZE Scenarios). Dedicated renewable production for low-carbon hydrogen represents more than 10% of global electricity generation in the APS scenario by 2050 and 15% in the NZE Scenario. Large scale deployment of electrolytic hydrogen could bring down the costs of hydrogen production from electrolysis powered by decreasing the electricity costs with dedicated renewable capacities. An optimal ratio of renewable capacity to electrolyzer must also be considered to identify the potential minimum levelized cost of production of hydrogen.

International trade of hydrogen and its derivatives would allow taking advantage of differentials in renewable endowment and electricity costs between regions and lower energy system costs. The transportation and storage of hydrogen however raise several technological, safety and economic issues, due to its low energy density, high flammability and propensity to leak. Hydrogen may

either be transported as compressed gas via pipeline or shipped as liquefied hydrogen and can be more conveniently distributed after conversion to synthetic fuels or combined with alternative carriers:

- **Gaseous Hydrogen (GH₂):** gaseous hydrogen produced can be injected directly into a pipeline and transported for different distances with new hydrogen pipelines and/or retrofitted natural gas pipelines. The pressure of compressed gaseous H₂ varies between 350 bar and 700 bar, corresponding to a volumetric mass density of 23 kg/m³ and 42 kg/m³ respectively (IRENA, 2022). The cost of pipelines varies in function of the distance, the flow transported and energy consumption for re-compression requirements due to the pressure losses. Currently, only small hydrogen pipeline grids exist to supply industrial consumers (IRENA, 2022, Hank et al., 2023).
- **Liquefied Hydrogen (LH₂):** there exists currently two possible solutions for transporting Liquid Hydrogen (LH₂) with infrastructure adapted to its cryogenic characteristics: maritime (tanks) or road (cryogenic tankers). Hydrogen liquefaction offers the advantage of higher storage and transport efficiency, with a density of 71 kg/m³, yet require cooling hydrogen to below -252.87 °C. The maritime transport of LH₂ transport technology thus requires tanks specially designed to resist extremely low temperatures and advanced thermal insulation to limit losses through evaporation or "boil-off". Currently, no large-capacity LH₂ transport vessel is in service (only the Suiso-Frontier, the first liquid hydrogen carrier, is operational with a capacity of 8000 tonnes).
- **Methanol (CH₃OH):** as a compound of carbon dioxide and hydrogen, methanol is in liquid phase at room temperature, and exhibits a very high density of 792 kg/m³. Although its combustion releases CO₂, the CO₂ used for its synthesis can be sources from CCS (carbon capture and storage) or biomass.
- **Ammonia (NH₃):** especially used for fertilizer production, the maritime transport of ammonia in liquid form is already a mature technological option (see Erdemir and Dincer, 2024), with ship design adapted to the toxicity and corrosion properties of NH₃. As a compound of hydrogen and nitrogen, ammonia offers significant benefits for storage and transportation, with a boil-off point below 33 °C and a volumetric mass density of 682 kg/m³. The demand for ammonia is expected to grow in future years, especially for international transport by sea.
- **Liquid Organic Hydrogen Carrier (LOHC):** considered as a large-scale hydrogen transport solution for international trade of hydrogen, this solution has not yet been deployed due to multiple obstacles. Despite the advantage of limiting the boil-off losses during the transport and using existing infrastructure, multiple obstacles still exist as low hydrogen content

and the need to transport a large mass of LOHC, high energy consumption and high temperature heat for dehydrogenation (IRENA, 2022).

Osman et al., 2024 provide a comprehensive discussion of the advantages, disadvantages and challenges of the implementation of alternative fuels such as hydrogen, ammonia and methanol for marine transportation. Conversion to hydrogen derivatives (ammonia, methanol and e-fuels) would help to overcome the low volumetric energy density issue, but imposes stringent handling and storage constraints, in addition to conversion losses and economic inefficiencies. Moreover, maritime transportation of hydrogen and its derivatives requires adaptation of existing export and import harbours in terms of infrastructure adequacy, risk management, regulations and standards. In addition, international trade of hydrogen and its derivatives also raises regulatory issues regarding the harmonization of the definitions used to distinguish various types of hydrogen based on their production method and carbon content, standards and green hydrogen certification schemes.

Few studies on the modeling of the low-carbon hydrogen value chain focus on the international trade aspect and the role that the establishment of infrastructures dedicated to the transport of these molecules could play in terms of reducing energy supply costs, mitigating energy transition costs for "hard-to-abate" sectors and meeting GHG reduction targets (Lullo et al., 2022, Fattahi et al., 2024). Moritz et al., 2023 evaluate the total supply costs of H₂-derivatives to Germany considering both pipeline-based and maritime transport and the geographic distribution of production and supply costs (113 countries). By applying a linear optimisation framework, the developed model calculates the minimum Levelised Cost of Supply of conventional hydrogen and synthetic hydrogen-based energy commodities (ammonia, methanol, methane and Fischer-Tropsch liquids). They find that production costs dominate the supply cost composition for liquefiable commodities, while transportation costs dominate for gaseous commodities. In the case of Germany, importing green ammonia could be more cost-efficient than domestic production from locally produced or imported hydrogen specially if imported hydrogen, from Spain, for ammonia production, is done with repurposed natural gas pipelines. Nonetheless, as pointed out by Moritz et al., 2023, for country-level resolution, the model suppose the transport from the capital to the relevant port which can bias the real transport costs.

In a recent work, Klaas et al., 2024 provide scenarios regarding the development of the global supply of green hydrogen and hydrogen derivatives (ammonia, methane, methanol and Fischer-Tropsch-fuel) from only wind and solar energy using the EWI Global PtX Cost Tool². The tool enables the analysis of production costs including storage for 117 countries and the transportation costs to 19 destination countries for different demand profiles (annual, hourly and volatile) with pipelines or by sea routes. The model minimizes produc-

²<https://www.ewi.uni-koeln.de/en/tools/globales-ptx-produktions-und-importkostentool/>

tion costs and considers the cheapest possible transportation alternatives with specific assumptions on the evolution of investment cost for pipelines, regasification, liquefaction and reconversion plants. Daiyan et al., 2021 developed the HySupply Shipping Analysis Tool³ to model the cost of shipping hydrogen between Australian and global ports to those in Europe and Asia for liquid hydrogen (LH2) and hydrogen carriers (ammonia, methanol, methane (LNG) and LOHC (as toluene / methylcyclohexane)). Modeling of maritime transport costs include ship investment, storage investment, labour, canal use charges, port service charges, maintenance, insurance, storage operating costs, fuel, carbon emissions and BOG costs. The total energy delivered is dependent on the storage capacity of the vessel (in tonnes) and the number of trips made per year, which in turn is influenced by the ship speed, shipping route length, time spent docked at port and ship availability for operation (days/year). Johnston et al., 2022 evaluate the shipping costs associated to various energy carriers and show that ammonia is the cheapest hydrogen carrier, closely followed by methanol. LNG, LOHC (TOL/MCH), and LH2 are all significantly more expensive. However, the methodology has two limitations in calculating transportation costs, which do not include upstream and downstream costs related to hydrogen conversion and reconversion, and also in the modeling framework adopted, which is formulated as a set of mathematical equations without optimization of investment and operating decisions.

In Alanazi et al., 2025, the authors combine a global modeling framework using TIMES model, incorporating hydrogen demand and supply curves, with a market equilibrium model. They compare an unrestricted trade scenario, allowing for hydrogen trade between all regions globally, and a regional independence scenario where trade is restricted to inter-regional exchanges. Considering LH2, NH3 and LOHC as potential energy carriers, they calculate unit transportation costs in \$/kgH2 using distances from the CERDI sea distances database⁴, which sums unit costs from conversion, storage at the export terminal, shipping, storage at the import terminal and reconversion. The unit cost corresponding to each step is expressed in MUSD/Mt H2/year, such that the total unit costs scales linearly with the volume of trade and fails to capture non-linearities stemming from the discrete nature of investment in conversion, storage and transportation units.

By modeling the sourcing of chemical feedstocks, synthesis and transportation for nine different Energy Supply Chains (ESCs), Hampp et al., 2023 compare import options for chemical energy carriers to Germany from seven locations against domestic alternatives. To account for the non-continuous and non-instantaneous nature of shipping delivery flows, the authors create *ex ante* shipping schedules with lowered cruise speeds to avoid overlapping uses of loading and unloading infrastructure by different groups of ships. However, the methodology used for computing shipping schedules is not explicitly presented.

³<https://www.globh2e.org.au/shipping-cost-tool>

⁴<https://ferdi.fr/en/indicators/the-cerdi-seadistance-database>

In addition, the authors rely on simplified transport assumptions, using representative average transportation costs that only scale with distance.

In a multi-commodity partial equilibrium model of future global hydrogen supply chains, Barner, 2024 introduces a techno-economic model of oligopolistic trade formulated as a Mixed Complementarity Problem (MCP). This paper noticeably accounts for barriers to market entry associated with the high capital intensity of initial investments in the early-stages of hydrogen supply chains. The MCP formulation is however linear and thus does not reflect the discrete nature of investment and operational shipping decisions. Although the author manages to express non-linear relationships by piece-wise approximations combining linear and quadratic terms, transportation constraints and costs are poorly represented.

Introduced by Nuñez-Jimenez and De-Blasio, 2022, MIGHTY (Model of International Green Hydrogen Trade) is an optimization model used to investigate the production, consumption and trade of renewable hydrogen between countries. Using a MILP formulation, it includes integer variables corresponding to the number of ships covering the trade route between each pair of countries, constrained by ship capacity, speed, maximum load, availability and fuel efficiency. Comparing LH2 and NH3 carriers, the transportation cost is calculated as the sum of conversion, storage, overseas shipping and reconversion costs. However, no integer variables are assigned the number of conversion and storage units, which capacity is estimated such that it satisfies requirements for continuous operations at the export and import terminals. Moreover, "to avoid mathematically correct but unrealistically small international hydrogen trades", minimum trade volumes of 10^3 , 10^4 and 10^5 kton/year are imposed for a trade route to be selected. MIGHTY thus does not allow the investigation of the early-stages of the hydrogen logistic transportation chain with low trade volumes. Moreover, as acknowledged by the authors, MIGHTY does not include short-term operational constraints, nor does it account for the overproduction requirements to compensate hydrogen losses from conversion and transportation.

By simultaneously minimizing total supply chain cost and CO2 emissions using a bi-objective optimization framework, Diamantis et al., 2024 present a comprehensive MILP model that determines the optimal choices of technologies, sizes and operational decisions for both the production and transportation of hydrogen under NH3 form. The numbers of vessels as well as their loading, departure and unloading are all modelled using integer variables, while the flows of vessels and H2 between exporting and importing regions are constrained by Kirchhoff laws. This compact formulation however requires an important number of integer variables, which leads to high computational times requiring time aggregation methods. Moreover, the model formulation does not distinguish NH3 storage and transportation units, which are used as mobile storage units when charging or discharging at the dock. Finally, although the proposed case study accounts for losses along that supply chain and assumes that a fraction of

the transported NH₃ is self-consumed by the vessels, these hypotheses do not feature in the model mathematical formulation.

From another perspective, focusing on the early stages of the hydrogen transport supply chain and its specific challenges for international trade, as explained by Cayet et al., 2024, bottom-up Hydrogen Supply Chain (HSC) design and planning optimisation models typically provide the most comprehensive modeling of HSC functional echelons and technical constraints, but fail to account for cooperation issues and strategic market interactions that influence investment decisions. Demand is often modelled as exogenous and deterministic, while demand uncertainty strongly affects expected stranded costs for infrastructure with high upfront costs, which is the case of maritime transport infrastructure. The quantification of investment risks associated with uncertain future hydrogen trade volumes and international cooperation issues is pivotal for the successful development of maritime transport infrastructure.

The present paper introduces a multi-regional, multi-commodity investment and operational optimization model to evaluate the levelised transportation cost of hydrogen and its derivatives for specific maritime trade routes. It is formulated as a MILP with both annual investment and daily operational decisions, covering conversion, export terminal storage, transportation, import terminal storage and reconversion flows. Our model both accounts for stock and flow constraints, and includes factors influencing transportation costs identified in the literature such as maritime distance, port charges and canal fees, ship size and required power, fuel consumption and boil-off gas (BOG) losses. Similarly to Diamantis et al., 2024, we keep track of the number of vessels used for shipping using integer variables, with explicit constraints on fuel requirements for ships using their own cargo for propulsion. Our model, coupled with a comprehensive cost decomposition, allows us to track non-linearities in the dynamics of cost categories and economies of scale for extremely low to large import volumes of hydrogen and its derivatives. This allows us to derive the minimum efficient scale for specific maritime trade routes and provide a precise decomposition of the share of each cost category in the total cost for various trade volumes, in addition to their allocation between exporting and importing regions. Consistent with Chen et al., 2025 and Schuler et al., 2024, we find a consistent transportation cost differential in favour of NH₃ when compared to LH₂, even when accounting for the extra-cost associated to the conversion and reconversion of hydrogen to and from NH₃. Finally, we provide a short econometric analysis of the effects of a subset of exogenous parameters identified in the literature on hydrogen transportation cost.

1 H2-derivatives Maritime Transport model

1.1 Theoretical Formalization

1.1.1 Parameters and Variables

- **Indices and sets:**

The transportation logistic chain can be decomposed into four technical echelons, associated to distinct subsets of technologies. First, C_1 corresponds to the conversion echelon in exporting countries, while S_1 corresponds to the storage step post-conversion. T is the transportation echelon, followed by a storage step S_2 and a reconversion step C_2 in importing countries. We assume storage technologies used in both storage echelons are identical, such that $\mathcal{T}_{S_1} = \mathcal{T}_{S_2} \triangleq \mathcal{T}_S$.

Our model is defined using a daily time step resolution over a whole year, such that operational decisions regarding hydrogen production, conversion, storage, transportation and reconversion are taken on a daily basis. Regarding the set of geographical regions \mathcal{R} , while each region may both be considered an exporter or an importer, we will assume for simplicity that a given region cannot simultaneously export and import energy products, such that $\mathcal{R}^X \cap \mathcal{R}^M = \emptyset$. Table 1 below provides an overview of definitions and notations for sets and mappings used in our model.

Set/Mapping	Description
\mathcal{J}	Set of all days j
\mathcal{P}	Set of all energy products p
\mathcal{C}	Set of all commodities used by technological processes c
\mathcal{R}	Set of all geographical regions r
\mathcal{R}^X	Subset of exporting geographical regions
\mathcal{R}^M	Subset of importing geographical regions
\mathcal{T}	Set of all available technologies t
\mathcal{T}_{C_1}	Subset of available conversion technologies
\mathcal{T}_S	Subset of available storage technologies
\mathcal{T}_T	Subset of available transportation technologies
\mathcal{T}_{C_2}	Subset of available reconversion technologies
$\mathcal{P}(t)^{-1}$	Mapping of energy products associated to technology $t \in \mathcal{T}$
$\mathcal{C}(t)^{-1}$	Mapping of commodities associated to technology $t \in \mathcal{T}$
$\mathcal{T}_{C_1}(\{p, p'\})^{-1}$	Mapping of conversion technologies associated to energy products $(p, p') \in \mathcal{P} \times \mathcal{P}$
$\mathcal{T}_{C_2}(\{p, p'\})^{-1}$	Mapping of reconversion technologies associated to energy products $(p, p') \in \mathcal{P} \times \mathcal{P}$
$\mathcal{T}_T(p)^{-1}$	Mapping of transportation technologies associated to energy product $p \in \mathcal{P}$

Table 1: Summary table of model sets and mappings

The use of mappings allows us to uniquely associate subsets of two distinct sets, and thus provides flexibility in modeling. For instance, as each technology in the transportation logistic chain can be associated to a unique subset of energy products, there exists an application (not necessarily injective) $\mathcal{P}: t \mapsto \mathcal{P}(t)^{-1}$ which assigns t to the subset \mathcal{P} .

- **Parameters:**

They can be decomposed into cost and general economic parameters, physico-chemical parameters, technological parameters and general technical parameters. For consistency, we define energy products consumption, production and unit capacities in tons, such that we keep track of the mass of energy products throughout the transportation supply chain. While capacities are usually specific in volumetric units, we use the volumetric mass ρ_p to systematically convert the volumetric capacity of technologies to tons.

For any couple of energy products $(p, p') \in \mathcal{P} \times \mathcal{P}$, there exists a unique conversion or reconversion technology that converts p to p' , so that we can equivalently define the conversion efficiency $\eta_{p,p',t}$ as η_t . The mass conversion rate $\mu_{p,p',t}$ is taken from Scheffler et al., 2025, with a value of 0.179 kgH₂/kgNH₃ for the conversion of hydrogen to ammonia. The conversion efficiency measures the ratio between the quantity of energy (in MJ) per kilogram of output product p' and the quantity of energy per kilogram of input product p . It is computed as follows:

$$\eta_t \triangleq \eta_{p,p',t} = \frac{L_{p'}}{L_p} \times \frac{1}{\mu_{p,p',t}}$$

As our model simultaneously optimises investment and operational decisions over an entire year, the investment cost $C_{r,t}^I$ and FOM cost $C_{r,t}^{FOM}$ must be annualized for economic consistency. Using above definitions, the annuity $A_{r,t}$ corresponding to stationary technology $t \in \mathcal{T} \setminus \mathcal{T}_T$, and the annuity $A_{r,r',t}$ for transportation technology $t \in \mathcal{T}_T$, are respectively computed as follows:

$$A_{r,t} = C_{r,t}^I \times \left[\frac{w_{r,t}}{1 - (1 + w_{r,t})^{-l_t}} \right]$$

$$A_{r,r',t} = C_{r,r',t}^I \times \left[\frac{w_{r,t}}{1 - (1 + w_{r,t})^{-l_t}} \right]$$

Similarly, for each transportation technology $t \in \mathcal{T}_T$, we can compute its hourly fuel consumption in MJ and convert it to daily mass consumption of fuel γ_t^F as follows, where $\{p\} \in \mathcal{P}(t)^{-1}$:

$$\gamma_t^F = 10^3 \times 24 \times 3.6 \times \left(\frac{\kappa_t^M}{\eta_t^M L_t^F} + \frac{\kappa_t^P}{\eta_t^P L_t^F} \right)$$

Where by convention, $L_t^F = L_p$ if the fuel used by transportation technology t corresponds to an energy product p . For transportation technologies fueled by conventional marine fuels, we assumed the BOG is entirely reliquefied and reliquefaction energy requirements are included into onboard ship services. Finally, for a given couple of exporting and importing regions $(r, r') \in \mathcal{R}^X \times \mathcal{R}^M$, the total round-trip duration for transportation technology $t \in \mathcal{T}_T$ is calculated as follows:

$$\tau_{r,r',t} = 2\lceil \delta_{r,r'} v_t^{-1} \rceil + (\tau_r^H + \tau_{r'}^H) + (\tau_r^B + \tau_{r'}^B)$$

For all transportation technologies, the flash rate is defined by the IEA (see International Energy Agency, 2024a) as the rate of loss that occurs upon each loading/unloading of cryogenic liquefied gas. For simplicity, we assume that the one-way travel duration $\delta_{r,r'} v_t^{-1}$ is rounded to the smallest integer superior or equal to it, so that the total round-trip duration is an integer number of days.

Table 2 below provides an overview of definitions and notations for parameters that are used in the model.

Parameter	Description
$C_{r,t}^I(C_{r,r',t}^I)$	Overnight investment cost for technology $t \in \mathcal{T} \setminus \mathcal{T}_T$ (resp. $t \in \mathcal{T}_T$) and region $r \in \mathcal{R}$ [in k\$]
$C_{r,t}^{FOM}(C_{r,r',t}^{FOM})$	FOM cost for technology $t \in \mathcal{T} \setminus \mathcal{T}_T$ (resp. $t \in \mathcal{T}_T$) and region $r \in \mathcal{R}$ [in k\$]
$A_{r,t}$	Annuity of stationary technology $t \in \mathcal{T} \setminus \mathcal{T}_T$ and region $r \in \mathcal{R}$ [in k\$]
$A_{r,r',t}$	Annuity of transportation technology $t \in \mathcal{T}_T$ and regions $(r, r') \in \mathcal{R} \times \mathcal{R}$ [in k\$]
$C_{r,c}$	Unit cost of commodity $c \in \mathcal{C}$ and region $r \in \mathcal{R}$ [in k\$/MWh]
$C_{r,t}^F$	Unit fuel cost for transportation technology $t \in \mathcal{T}_T$ and region $r \in \mathcal{R}$ [in k\$/ton]
$C_{r,r'}^C$	Canal-crossing cost from region $r \in \mathcal{R}$ to $r' \in \mathcal{R}$ [in k\$/ton]
C_r^H	Port charges in region $r \in \mathcal{R}$ [in k\$/day]
$\pi_r^{CO_2}$	Carbon cost for region $r \in \mathcal{R}$ [in k\$/ton]
$w_{r,t}$	Weighted average capital cost for technology $t \in \mathcal{T}$ and region $r \in \mathcal{R}$
l_t	Economic lifetime duration of technology $t \in \mathcal{T}$ [in years]
$d_{j,r}$	Consumption of energy product $p \in \mathcal{P}$ for day $j \in \mathcal{J}$ and region $r \in \mathcal{R}$ [in kton]
ρ_p	Volumic mass of energy product $p \in \mathcal{P}$ [in kg/m ³]
$\mu_{p,p',t}$	Mass conversion rate for technology $t \in \mathcal{T}_{C_1} \cup \mathcal{T}_{C_2}$ and products $(p, p') \in \mathcal{P} \times \mathcal{P}$ [in kg _p /kg _{p'}]
L_p	Lower Heating Value (LHV) of energy product $p \in \mathcal{P}$ [in MJ _p /kg _p]
L_t^F	Lower Heating Value (LHV) of fuel for transportation technology $t \in \mathcal{T}_T$ [in MJ/kg]
$\eta_{p,p',t}$	Conversion efficiency for technology $t \in \mathcal{T}_{C_1} \cup \mathcal{T}_{C_2}$ and products $(p, p') \in \mathcal{P} \times \mathcal{P}$ [in %]
β_t^1	Boil-off gas (BOG) rate for storage or transportation technology $t \in \mathcal{T}_S \cup \mathcal{T}_T$ [in ton/day]
β_t^2	Flash rate for transportation technology $t \in \mathcal{T}_T$ [in %]
\bar{K}_t	Nominal capacity for technology $t \in \mathcal{T}$ [in ton or ton/day]
v_t	Average speed for transportation technology $t \in \mathcal{T}_T$ [in km/day]
$\kappa_t^M(\kappa_t^P)$	Engine (resp. ship service) power requirements for transportation technology $t \in \mathcal{T}_T$ [in MW]
$\eta_t^M(\eta_t^P)$	Engine (resp. ship service) efficiency for transportation technology $t \in \mathcal{T}_T$ [in %]
E_t	Carbon intensity of fuel for transportation technology $t \in \mathcal{T}_T$ [in tonCO ₂ /ton]
γ_t^F	Fuel consumption of transportation technology $t \in \mathcal{T}_T$ [in ton/day]
$\gamma_{t,c}$	Consumption of commodity $c \in \mathcal{C}$ by technology $t \in \mathcal{T}$
$\delta_{r,r'}$	Sea distance between regions $(r, r') \in \mathcal{R} \times \mathcal{R}$ [in km]
τ_r^B	Berthing time for region $r \in \mathcal{R}$ [in days]
τ_r^H	Queuing time at harbor entry in region $r \in \mathcal{R}$ [in days]
$\tau_{r,r',t}$	Total round-trip duration for technology $t \in \mathcal{T}_T$ between regions $(r, r') \in \mathcal{R} \times \mathcal{R}$ [in days]

Table 2: Summary table of model parameters

- **Decision variables:**

The investment variables $U_{r,t}^1$ and $U_{r,r',t}^2$ are defined as integer variables and thus correspond to a discrete number of technological units. We implicitly assume through the above formulation that each transportation unit is assigned to a unique maritime route between regions r and r' for its entire economic lifetime. To avoid confusion, we distinguish the conversion fluxes $\overrightarrow{\Gamma}_{j,r,t}$ from reconversion fluxes $\overleftarrow{\Gamma}_{j,r,t}$, as only an energy product that has been first converted and transported from an exporting region can be reconverted in an importing region. The condition that \mathcal{R}^X and \mathcal{R}^M are disjoint is thus equivalent to the constraints $\overrightarrow{\Gamma}_{j,r',t} = 0$ and $\overleftarrow{\Gamma}_{j,r,t} = 0$.

Finally, we introduce the integer variables $X_{j,r,r',t}$ to keep track of the daily number of ships leaving from region r to region r' .

Decision variable	Description
$U_{r,t}^1 \in \mathbb{N}$	Number of units for stationary technology $t \in \mathcal{T} \setminus \mathcal{T}_T$ and region $r \in \mathcal{R}$
$U_{r,r',t}^2 \in \mathbb{N}$	Number of units for transportation technology $t \in \mathcal{T}_T$ and region $r \in \mathcal{R}$
$\Omega_{j,r,t} \in \{0,1\}$	State of charge for storage technology $t \in \mathcal{T}_S$, day $j \in \mathcal{J}$ and region $r \in \mathcal{R}$
$s_{j,r,t} \in \mathbb{R}^+$	Energy stock for storage technology $t \in \mathcal{T}_S$, day $j \in \mathcal{J}$ and region $r \in \mathcal{R}$ [in tons]
$s_{j,r,t}^+ \in \mathbb{R}^+$	Energy inflow for storage technology $t \in \mathcal{T}_S$, day $j \in \mathcal{J}$ and region $r \in \mathcal{R}$ [in tons]
$s_{j,r,t}^- \in \mathbb{R}^+$	Energy outflow for storage technology $t \in \mathcal{T}_S$, day $j \in \mathcal{J}$ and region $r \in \mathcal{R}$ [in tons]
$q_{j,r} \in \mathbb{R}^+$	Gaseous H_2 production for day $j \in \mathcal{J}$ and region $r \in \mathcal{R}$ [in tons]
$\overrightarrow{\Gamma}_{j,r,t} \in \mathbb{R}^+$	Quantity converted by technology $t \in \mathcal{T}_{C_1}$ for day $j \in \mathcal{J}$ and region $r \in \mathcal{R}$ [in tons]
$\overleftarrow{\Gamma}_{j,r,t} \in \mathbb{R}^+$	Quantity (re)converted by technology $t \in \mathcal{T}_{C_2}$ for day $j \in \mathcal{J}$ and region $r \in \mathcal{R}$ [in tons]
$T_{j,r,r',t} \in \mathbb{R}^+$	Quantity exported on day $j \in \mathcal{J}$ for technology $t \in \mathcal{T}_T$ from region $r \in \mathcal{R}$ to $r' \in \mathcal{R} \setminus \{r\}$ [in tons]
$X_{j,r,r',t} \in \mathbb{N}$	Number of ships of technology $t \in \mathcal{T}_T$ leaving on day $j \in \mathcal{J}$ from region $r \in \mathcal{R}$ to $r' \in \mathcal{R} \setminus \{r\}$

Table 3: Summary table of model decision variables

1.1.2 Objective Function

The optimal investment and dispatch transportation problem introduced in this paper can be described as a cost-minimization problem and is described as a MILP. For a given set of geographical regions, we minimize the aggregated sum of investment costs, formulated as annuities, and of annual operational costs. Formally, we minimize the expression described in equation (1):

$$\min_{\substack{\mathbf{U}^1, \mathbf{U}^2, \overrightarrow{\Gamma}, \overleftarrow{\Gamma}, \mathbf{q} \\ \Omega, \mathbf{s}^+, \mathbf{s}^-, \mathbf{T}, \mathbf{X}}} \sum_{r \in \mathcal{R}} \left(C_r^1 + C_r^2 + \sum_{r' \in \mathcal{R} \setminus \{r\}} C_{r,r'}^3 + C_{r,r'}^4 \right) \quad (1)$$

such that equations (1a) to (12) listed and described below are verified :

$$C_r^1 = \sum_{t \in \mathcal{T} \setminus \mathcal{T}_T} (A_{r,t} + C_{r,t}^{FOM}) U_{r,t} + \sum_{t \in \mathcal{T}_T} \sum_{r' \in \mathcal{R} \setminus \{r\}} (A_t^{r,r'} + C_{r,r',t}^{FOM}) U_{r,r',t} \quad (1a)$$

$$C_r^2 = \sum_{j \in \mathcal{J}} \left(\sum_{t \in \mathcal{T}_C} \sum_{c \in \mathcal{C}(t)^{-1}} C_{r,c} \gamma_{t,c} (\overrightarrow{\Gamma}_{j,r,t} + \overleftarrow{\Gamma}_{j,r,t}) + \sum_{t \in \mathcal{T}_S} \sum_{c \in \mathcal{C}(t)^{-1}} C_{r,c} \gamma_{t,c} s_{j,r,t} \right) \quad (1b)$$

$$C_{r,r'}^3 = \sum_{j \in \mathcal{J}} \left(\sum_{t \in \mathcal{T}_T} [C_r^H \tau_{p,r}^B + C_{r'}^H \tau_{p,r'}^B + 2C_{r,r'}^C + C_{r,t}^F \gamma_{t'}^F (\tau_{r,r',t'} - (\tau_r^B + \tau_{r'}^B))] X_{j,r,r',t} \right) \quad (1c)$$

$$C_{r,r'}^4 = \left(\frac{\pi_r^{CO_2}}{2} + \frac{\pi_{r'}^{CO_2}}{2} \right) \sum_{j \in \mathcal{J}} \sum_{t \in \mathcal{T}_T} \gamma_t^F E_t (\tau_{r,r',t'} - (\tau_r^B + \tau_{r'}^B)) X_{j,r,r',t} \quad (1d)$$

The total cost in (1) can indeed be decomposed into four cost categories. (1a) corresponds to the sum of annuities and FOM costs for both stationary and transportation technologies. C_r^2 in (1b) is equal to the aggregated yearly cost of commodities required for conversion, reconversion and storage processes in region $r \in \mathcal{R}$. For a given couple of regions $r \in \mathcal{R}^X \times \mathcal{R}^M$, $C_{r,r'}^3$ in (1c) corresponds to the total aggregated cost associated to the maritime route between the two regions. It is equal to the sum of port charges, canal-crossing charges (if the route between r and r' required crossing the Suez or Panama canal) and fuel costs, multiplied by the total number of ships rotations over the year. Finally, equation (1d) is equal to the aggregate CO2 cost associated to transportation flows between r and r' over the year. We define the carbon price is equal to the average price between the exporting and importing regions. Thus, even regions which apply no carbon tax have 50 % of their carbon emissions generated by ship transportation taxed at the CO2 price of the exporting/importing region. This is similar in spirit to the EU's Carbon Border Mechanism Adjustment (CBAM), which coverage has been extended to the maritime sector on 1 January 2024: under this system, 100 % of carbon emissions generated during journeys within the EU are taxed, while 50 % of emissions from trips from or to non-EU countries are taxed.

1.1.3 Technical constraints

Conversion technologies in exporting regions $r \in \mathcal{R}^X$ are subjected to a **capacity constraint**, such that the quantity of energy product p that can be converted to p' must be inferior or equal to the capacity of conversion technology t :

$$\overrightarrow{\Gamma}_{j,r,t} \leq U_{r,t}^1 \overleftarrow{K}_t \quad (2)$$

Similarly for importing regions $r' \in \mathcal{R}^M$ and for any reconversion technology $t \in \mathcal{T}_{C_2}$, the quantity of energy product p that can be reconverted to p' , where $\{p, p'\} \in \mathcal{P}(t)^{-1}$, is limited by the following **capacity constraint**:

$$\overleftarrow{\Gamma}_{j,r',t} \leq U_{r',t}^1 \overline{K}_t \quad (3)$$

The quantity of converted energy product is limited by a **flux constraint**: for any $p \in \mathcal{P}$, the total quantity that can be converted into product $p' \in \mathcal{P}$ must be inferior or equal to the daily production of hydrogen available $q_{j,r,p}$, such that:

$$\sum_{p' \in \mathcal{P}} \sum_{t \in \mathcal{T}_{C_1}(\{p,p'\})^{-1}} \overrightarrow{\Gamma}_{j,r,t} \leq q_{j,r,p} \quad (4)$$

Similarly, we define a **capacity constraint** on the quantity of energy product that can be stored in storage technology $t \in \mathcal{T}_S$:

$$s_{j,r,t} \leq U_{r,t}^1 \overline{K}_t \quad (5)$$

We further introduce a **stock constraint** on storage dynamics, and use the binary variable $\Omega_{j,r,t}$ associated to the large scalar $M \gg 0$ (big-M method) to prevent storage units from simultaneously loading and unloading :

$$s_{j,r,t} = s_{j-1,r,t} + s_{j,r,t}^+ - s_{j,r,t}^- - \beta_t^1 \quad (5a)$$

$$s_{j,r,t}^+ \leq \Omega_{j,r,t} M \quad (5b)$$

$$s_{j,r,t}^- \leq (1 - \Omega_{j,r,t}) M \quad (5c)$$

Following (5a), the variation of storage stock between two consecutive days is equal to inflows $s_{j,r,t}^+$ minus outflows $s_{j,r,t}^-$ and storage losses. The introduction of the binary variable $\Omega_{j,r,t}$ is a cautionary move to avoid the existence of null storage capacity requirements from inflows and outflows happening simultaneously. This issue is however unlikely to occur if the inflow of converted product is constant. We further introduce a **flux constraint** imposing equality on inflows into storage units in exporting region $r \in \mathcal{R}^X$ for storage technology $t \in \mathcal{T}_S$ and the total quantity of energy product, accounting for conversion efficiency:

$$\sum_{p' \in \mathcal{P}(t)^{-1}} \left(\sum_{p \in \mathcal{P}} \sum_{t' \in \mathcal{T}_{C_1}(\{p, p'\})} \eta_{t'} \overrightarrow{\Gamma}_{j, r, t'} \right) = s_{j, r, t}^+ \quad (6)$$

Likewise, for importing region $r' \in \mathcal{R}^M$, we impose a **flux constraint** linking the outflow from storage units for storage technology $t \in \mathcal{T}_S$ and the total quantity of energy product $p \in \mathcal{P}(t)^{-1}$ injected into available reconversion technologies:

$$\sum_{p \in \mathcal{P}(t)^{-1}} \left(\sum_{p' \in \mathcal{P}} \sum_{t' \in \mathcal{T}_{C_2}(\{p, p'\})} \frac{1}{\eta_{t'}} \overleftarrow{\Gamma}_{j, r', t'} \right) = s_{j, r', t}^- \quad (7)$$

For transportation technology $t \in \mathcal{T}_T$, the quantity of energy product that can be transported in $j \in \mathcal{J}$ from exporting region r to r' is subjected to a **dynamic capacity constraint**, such that it must be inferior or equal to the transportation capacity remaining in port:

$$T_{j, r, r', t} \leq \overline{K}_t X_{j, r, r', t} \quad (8)$$

Equation (8) is complemented by auxiliary equations (8a-8b), where the former corresponds to a **dynamic capacity constraint** such that $X_{j, r, r', t}$ must be inferior or equal to the number of ships remaining in exporting port. This capacity is equal to the difference between total number of vessels $U_{r, r', t}^2$ and the number of ships that have left the port and not completed a full rotation. (8b) specifies the initial conditions by constraining $X_{j, r, r', t}$ to be inferior or equal to the total transportation capacity at the beginning of the period.

$$X_{j, r, r', t} \leq U_{r, r', t}^2 - \sum_{j'=1}^{j \wedge \tau_{r, r', t}} X_{j-j', r, r', t} \quad (8a)$$

$$X_{j, r, r', 1} \leq U_{r, r', t}^2 \quad (8b)$$

In exporting countries $r \in \mathcal{R}^X$, pre-transportation storage units and transportation units are linked by a **flux constraint**, such that for any storage technology $t \in \mathcal{T}_S$ and day $j \in \mathcal{J}$, the outflow of energy product

$\{p\} \in \mathcal{P}(t)^{-1}$ must be equal to total quantity transported by technologies $t' \in \mathcal{T}_T(p)^{-1}$ to different exporting regions, accounting for loading duration:

$$\sum_{r' \in \mathcal{R}^M} \left(\sum_{p \in \mathcal{P}(t)^{-1}} \sum_{t' \in \mathcal{T}_T(p)^{-1}} T_{j,r,r',t'} \right) = s_{j-\tau_r^B,r,t}^- \quad (9)$$

For importing region $r' \in \mathcal{R}^M$, the following equation models the **flux constraint** linking inflows into storage technology $t \in \mathcal{T}_S$ and the total quantity of energy product $p \in \mathcal{P}(t)^{-1}$ imported from exporting regions:

$$\sum_{r \in \mathcal{R}^X} \left(\sum_{p \in \mathcal{P}(t)^{-1}} \sum_{t' \in \mathcal{T}_T(p)^{-1}} (1 - \beta_{t'}^2) \left[(1 - \beta_{t'}^2) T_{j-\overrightarrow{\tau_{r,r',t'}},r,r',t'} - \gamma_{t'}^F (\tau_{r,r',t'} - (\tau_r^B + \tau_{r'}^B)) X_{j-\overrightarrow{\tau_{r,r',t'}},r,r',t'} \right] \right) = s_{j,r',t}^+ \quad (10a)$$

For the case of transportation units using conventional marine fuels for propulsion, under the assumption that all BOG is re-liquefied onboard, the **flux constraint** is expressed as follows:

$$\sum_{r \in \mathcal{R}^X} \left(\sum_{p \in \mathcal{P}(t)^{-1}} \sum_{t' \in \mathcal{T}_T(p)^{-1}} (1 - \beta_{t'}^2)^2 T_{j-\overrightarrow{\tau_{r,r',t'}},r,r',t'} \right) = s_{j,r',t}^+ \quad (10b)$$

For transportation technologies using their own cargo for propulsion, equation (11) below ensures that the transported quantity $T_{j,r,r',t}$ is greater or equal to the fuel requirements for a complete round-trip between regions r and r' , accounting for flash rate losses:

$$-(1 - \beta_{t'}^2) T_{j,r,r',t'} \leq -\gamma_{t'}^F (\tau_{r,r',t'} - (\tau_r^B + \tau_{r'}^B)) X_{j,r,r',t'} \quad (11)$$

Finally, for importing regions $r' \in \mathcal{R}^M$, we impose that the annual aggregated quantity of energy products reconverted to energy product $p' \in \mathcal{P}$ by reconversion technologies \mathcal{T}_{C_2} is superior or equal to the annual demand for p' :

$$\sum_{j \in \mathcal{J}} \left(\sum_{p \in \mathcal{P}} \sum_{t' \in \mathcal{T}_{C_2}(\{p,p'\})} \overleftarrow{\Gamma}_{j,r',t'} \right) \geq \sum_{j \in \mathcal{J}} d_{j,r',p'} \quad (12)$$

1.1.4 Modeling assumptions

Several remarks are necessary regarding the application of the model developed in this paper.

First, it is an *static* investment model, as the investment decisions over available technologies are only made once. The model returns the optimal infrastructure and operational decisions required to satisfy the annual demand for energy product p (hydrogen in our case) in importing regions, which is set exogenously by the modeler. It assumes no initial capacities. However, this limitation can easily be addressed by using a multi-year framework and adding dynamic capacity constraints, although it may greatly increase model complexity and solution time.

Second, transportation capacities are by assumption assigned to a specific and unique maritime route. For instance, assuming $U_{r,r',t} > 0$, the corresponding ships cannot be used for exports from region $r \in \mathcal{R}^X$ to region $r'' \in \mathcal{R}^M, r'' \neq r'$.

Third, we impose no *a priori* shape constraint on the hydrogen production or consumption profiles. More specifically, we allow the model to freely choose the optimal daily inflow $q_{j,r,p}$ of product $p \in \mathcal{P}$ into conversion units. Indeed, as operational decisions are optimized over a finite period of length $|\mathcal{J}|$, a finite number of trips is required to satisfy a given import volume. Imposing a constant hydrogen inflow into conversion units could reduce computation time but would overestimate storage requirements in exporting regions, because of the existence of an irreducible quantity of hydrogen or derived product not shipped to importing regions. It is however possible to include seasonal patterns and more generally dynamic constraints on hydrogen production (resp. consumption) by introducing a time-varying constraint on the maximum daily inflow of gaseous hydrogen in exporting regions (resp. minimum daily outflow from storage units in importing regions).

Fourth, for a given importing region $r' \in \mathcal{R}^M$, the above model is formulated so as to allow imports from multiple exporting regions simultaneously. Conversely, a given exporting region $r \in \mathcal{R}^X$ can export to several importing regions. However, as our initial goal is to estimate the optimal transportation logistic chain infrastructure, unit cost and cost decomposition associated to each specific maritime route, we separately estimate the model for each pair $(r, r') \in \mathcal{R} \times \mathcal{R} \setminus \{r\}$. Equivalently, we specify the subsets \mathcal{R}^X and \mathcal{R}^M as singletons, with $\mathcal{R} = \mathcal{R}^X \cup \mathcal{R}^M$. Because of its additional analytic and computational complexity, we keep the estimation of optimal infrastructure with multiple exporters and/or importers of further research. It is however likely that the unit transportation cost associated to a given maritime route will be smaller when considering exports to multiple countries (resp. imports from multiple countries) due to additional economies of scale.

Finally, we use our model to estimate the optimal infrastructure and costs associated to each possible technological combination, even sub-optimal ones regarding total costs. Thus, we consider a single transportation technology at a time, such that \mathcal{T}_T is a singleton. It follows that equations (10a) and (10b) are not included simultaneously in the model.

1.2 Database and empirical assumptions

The construction of an integrated maritime H₂-derived database is based on CEA expertise, data collected through bibliographic research and online databases containing information on maritime infrastructure and seaports worldwide. The model’s database includes several categories: trade routes, maritime transport modes, hydrogen storage options, CO₂ emissions associated to each transport option, operational performance data and economic costs.

1.2.1 Routes and distances

The exploration and use of the WPI database⁵ allowed the identification of a set of ports eligible for the transport of H₂ and NH₃ (“WORLD PORT INDEX 150”, 2019). Our selection of ports was also based on Chen et al., 2023, who identify relevant candidate ports for international hydrogen trade, based on their degree of readiness (regarding existing or planned infrastructure, risk management, regulations, public acceptance). A dedicated Python code was developed to calculate different trade route alternatives between ports of countries/regions and to apply filters related to specific hypothesis choices such as the shortest distance or the average distance between two countries/regions. Another interesting aspect that this work has allowed to achieve is the possibility of identifying the geopolitical risk/danger points linked to certain maritime supply strategies (canals, straits, capes) and this according to each pair of ports.

1.2.2 Geographical coverage

Concerning geographical coverage, 7 countries are considered in this case study: France, Australia, China, Morocco, Brazil, the United-States and South Africa. This approach is motivated by the high solution time of the model, which imposes a limit on the number of candidate countries to be considered in our case study. Regarding selection criteria, our choice of countries is made so as to maximise the spread of exogenous model parameters (maritime distance, electricity cost, CO₂ cost, WACC) within the sample. This allows us to better capture the effect of these exogenous parameters on our results.

Pairwise maritime distances, as well as the average annual country prices of electricity and CO₂ prices, are reported in Table 4 and Table 5 in Appendix.

⁵<https://msi.nga.mil/Publications/DBP>

With an average value of 12,980 km, the pairwise maritime distance varies between 2,141 (France-Morocco) to 20,606 (China-Brasil). The price of electricity varies from 83 \$/MWh (Morocco) to 168 \$/MWh (South Africa), with an average value of 120 \$/MWh. Finally, the WACC ranges from 9.98 % (Australia) to 13.8 % (Brazil) and takes an average value of 11.77 %.

1.2.3 Technological and technical parameters

Several technologies are considered in our case study and are distinguished based on the following criteria: type of technology (conversion, storage, or maritime transport); energy carrier produced, stored, or transported; unit size capacity considering existing units worldwide; and fuel origin for propulsion and to produce facilities for ships. Regarding technical parameters used in the model, their description can be detailed as follows:

- **Conversion technologies:** the database includes one reference technology per type of conversion needed. This encompasses units that transform gaseous hydrogen into liquid form or ammonia, or reconvert it back into gaseous hydrogen. It's important to note that certain technologies, such as hydrogen liquefaction, do not yet exist at a large scale. All conversion technologies consume electricity, with potential minimal consumption even if there is no production. The heat production for ammonia dehydrogenation is produced by ammonia autoconsumption. The level of CO₂ emissions depends on the carbon content of electricity, which is linked to the electricity mix of the considered region as we assume electricity is entirely withdrawn from the power grid
- **Maritime transport technology:** Various maritime transport options are evaluated, first based on their capacity (medium-sized and large-sized, including those suitable for hydrogen), and secondly on their ability to use their own cargo for autoconsumption or conventional maritime fueling (MDO, i.e., marine diesel oil/HFO, i.e., heavy fuel oil). We distinguish the power requirements for propulsion and onboard auxiliary services, in addition to the power needed for onboard BOG reliquefaction if relevant. The total daily power requirement of each type of transportation unit is computed by adding these three components. We assume no reliquefaction for technologies using their own cargo for propulsion, as the BOG losses are entirely consumed and the remainder of daily power requirements not satisfied by BOG losses is directly extracted from the tanks. Finally, we assumed BOG losses are fully reliquefied onboard for transportation units using conventional maritime fuels for propulsion. For simplicity, we neglect the "slip" losses during shipping such that the theoretical engine speed of a vessel is equal to its observed speed. For all transportation, a 18 knots speed is considered. Our model only considers carbon emissions associated to the transportation flows between regions. We distinguish between MDO and HFO in terms of their LHV and carbon content to keep track of the emissions specific to each type of transportation unit.

We assume that the daily CO2 emissions are constant throughout a given journey, which may underestimate true emissions as carbon emissions are noticeably higher during the manoeuvre phase of vessels when entering and exiting ports.

- **Storage technologies:** technologies for storing liquid ammonia and liquid hydrogen in both export and import countries are considered. While large-scale hydrogen storage is not yet prevalent, a 160,000 m³ cylindrical storage is considered available for this study. Storage could also be concerned by BOG and consume electricity for reliquefaction when there is no possibility to recycle the gas into the main units (export countries).

1.2.4 Economic parameters

The main source of technical and economic data is the CEA studies (CAPEX, OPEX, capacity, required inputs and consumption per production unit, loss rates, etc.) and those of EWI (Hank et al., 2023), International Energy Agency, 2024a, I4CE Global Carbon Accounts and Ship Bunker for macroeconomic data (WACC, electricity/CO2 prices, fuels). A discrete modeling of the technological units is carried out with a differentiation by type of energy vector considered in input/output (GH2, LH2, NH3) and by size (medium/large for storage and transport units). With a total of 42 possible pairs of exporting and importing countries, 10 levels of hydrogen demand from imports (see Section 3.1. below) and 8 possible options for the transportation logistic chain, we executed a total of 3360 model runs.

2 International hydrogen trade case study

One of the primary objectives of this paper is to measure the Minimum Efficient Scale (MES) of the hydrogen transportation infrastructure, which corresponds to the minimum volume of imports such that the unit (or average) transportation cost equals the marginal transportation cost. This provides a measure of the minimum H2 trade flows required for a given maritime route to be economically viable. Note that the utilization rate of technologies are not reported but can be endogenously computed from our model results.

The concept of economies of scale refers to the decrease of unit cost arising from an increase of production and provides a natural measure of the MES.

2.1 Measuring the strength of economies of scale

Let us introduce a few notations: we define θ_r and $\theta_{r'}$ the vector of exogenous parameters (WACC, carbon cost, electricity cost, etc.) for exporting region $r \in \mathcal{R}^X$ and $r' \in \mathcal{R}^M$. For a given couple of regions $(r, r') \in \mathcal{R}^X \times \mathcal{R}^M$ and transportation technological pathway, we define $\mathbf{C}_{r,r'} = C_r^1 + C_r^2 + C_{r,r'}^3 + C_{r,r'}^4$ the corresponding total transportation cost and $\theta_{r,r'}$ the vector of associated

exogenous parameters (maritime distance, round-trip duration, canal-crossings fees).

For a given aggregated H2 demand in region $\mathbf{d}_{r'} \in \mathbb{R}^+$, we define the function $\mathbf{C}^* (\mathbf{d}_{r'} | \boldsymbol{\theta}_r, \boldsymbol{\theta}_{r'}, \boldsymbol{\theta}_{r,r'}) \triangleq \mathbf{C}_{r,r'}^* (\mathbf{d}_{r'}) : \mathbb{R}^+ \rightarrow \mathbb{R}^+$, which corresponds to the annual optimal total transportation cost. Economies of scale correspond to the situation where an increase in net hydrogen imports is met by a more than proportional decrease in unit transportation cost. For a given demand variation $\Delta \mathbf{d}$, they can be represented as a cost-production elasticity, by the function $\alpha_{r,r'} (\Delta \mathbf{d}) \in \mathbb{R}^+$ defined as follows:

$$\alpha_{r,r'} (\Delta \mathbf{d}) = \left(\frac{\mathbf{C}_{r,r'}^* (\mathbf{d}_{r'} + \Delta \mathbf{d}) - \mathbf{C}_{r,r'}^* (\mathbf{d}_{r'})}{\mathbf{C}_{r,r'}^* (\mathbf{d}_{r'})} \right) \times \left(\frac{\Delta \mathbf{d}}{\mathbf{d}_{r'}} \right)^{-1}$$

The function $\alpha_{r,r'} (\Delta \mathbf{d})$ can be easily computed from results and be interpreted as a measure of the strength of economies of scale when the annual net imported volume of hydrogen increases by $\Delta \mathbf{d}$ kton/year. Economies of scale correspond to the range $0 \leq \alpha_{r,r'} (\Delta \mathbf{d}) \leq 1$, while values superior to 1 indicate dis-economies of scale. $\alpha_{r,r'} (\Delta \mathbf{d})$ is thus equal to 1 when the minimum efficient scale is reached. However, to facilitate interpretations and comparisons between different values of net import volumes, we propose a dynamic definition of the exponent $\alpha_{r,r'} (\Delta \mathbf{d})$, allowing us to conveniently measure the dynamics of economies of scale.

In the following subsections, we investigate the transportation cost distribution and allocation for various volumes of annual hydrogen imports. Net import volumes are defined as powers of 2, such that for a given couple $(r, r') \in \mathcal{R}^X \times \mathcal{R}^M$, we double the volume of hydrogen arriving in importing region r' for each iteration. For $n \in \mathbb{N}^*$, let $\Delta_n = 2^n$ kton/year. The magnitude of economies of scale associated to an increase of imports volume from Δ_{n-1} to Δ_n , noted $\alpha_{r,r'}^n$, is then simply computed as follows, with the convention $\alpha_{r,r'}^1 = 0$:

$$\alpha_{r,r'}^n = \frac{\mathbf{C}_{r,r'}^* (\Delta_n) - \mathbf{C}_{r,r'}^* (\Delta_{n-1})}{\mathbf{C}_{r,r'}^* (\Delta_{n-1})}$$

Using this measure of economies of scale, it is possible to find an additive decomposition of the above expression to investigate their dynamics for each cost category separately. Defining $\mathbf{C}_{m,r,r'}^* (\Delta_n)$ as the cost associated to cost category $m \in \mathcal{M}$, the total cost variation can be decomposed as follows:

$$\mathbf{C}_{r,r'}^* (\Delta_n) - \mathbf{C}_{r,r'}^* (\Delta_{n-1}) = \sum_{m \in \mathcal{M}} \mathbf{C}_{m,r,r'}^* (\Delta_n) - \mathbf{C}_{m,r,r'}^* (\Delta_{n-1})$$

Thus:

$$\alpha_{r,r'}^n = \sum_{m \in \mathcal{M}} \left(\frac{\mathbf{C}_{m,r,r'}^*(\Delta_n) - \mathbf{C}_{m,r,r'}^*(\Delta_{n-1})}{\mathbf{C}_{r,r'}^*(\Delta_{n-1})} \right) = \sum_{m \in \mathcal{M}} \alpha_{m,r,r'}^n$$

where $\alpha_{m,r,r'}^n$ measures the economies of scale associated with cost category $m \in \mathcal{M}$ and an increase of the imported quantity from Δ_{n-1} to Δ_n .

Theoretically, there should be little economies of scale associated to variable OPEX cost categories, with the exception of transportation variable costs. Indeed, for a given maritime route and electricity prices in exporting and importing countries, this would imply that the quantity of hydrogen converted into LH2 or NH3 energy carriers and reconverted back to hydrogen would increase less than proportionally when the import volume increases. This either requires the existence of an excess production of hydrogen in exporting countries, which is converted and stored but not shipped to importing countries, or increased efficiency of technologies using LH2 or NH3 as input. On a side note, the existence of production surpluses may result from numerical issues associated to our choice of a 5 % relative optimality criterion (*relative gap*) with GAMS, which may lead to sub-optimal solutions.

Regarding transportation variable costs, they are directly proportional to the number of trips between regions r and r' , which may exhibit economies of scale if the average utilization rate of ships (measured by the ratio of $T_{j,r,r',t}$ and \overline{K}_t for a given trip and technology $t \in \mathcal{T}_T$) is below 100 %. As by assumption propulsion needs are independent of the quantity carried, the utilization rate of transportation units is expected to increase with import volume and as the number of trips per ship increases.

To rigorously assess these issues, let us define for a given transportation technology $t \in \mathcal{T}_T$ and couple of regions $(r, r') \in \mathcal{R}^X \times \mathcal{R}^M$ the minimum number of trips required between r and r' to satisfy net H2 demand $\mathbf{d}_{r'}$, noted $\chi_{r,r',t}(\mathbf{d}_{r'}) \in \mathbb{N}$, with $\chi_{r,r',t}(0) = 0$ by definition.

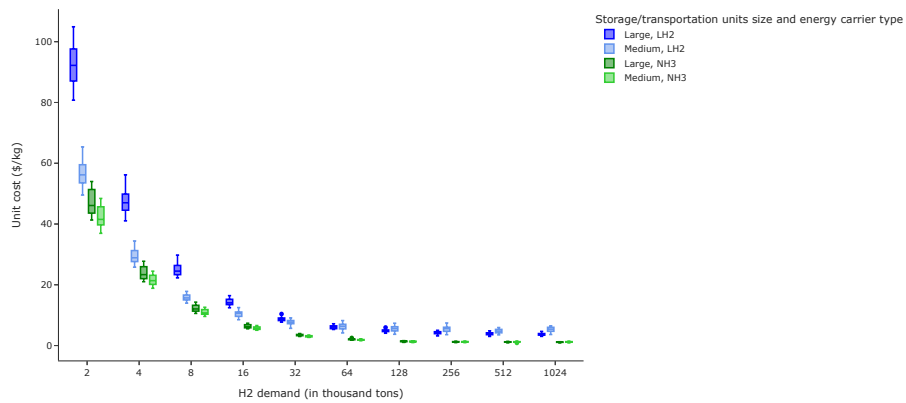
For a given imported quantity $\mathbf{d}_{r'}$, $\chi_{r,r',t}(\mathbf{d}_{r'})$ is itself non-decreasing with the round-trip duration $\tau_{r,r',t}$, as it increases fuel requirements and diminishes net payload by trip. The minimum number of trips required is thus the smallest integer that satisfies the following constraint, with $t' \in \mathcal{T}_{C_2}(p, \cdot), p \in \mathcal{P}(t)^{-1}$:

$$\chi_{r,r',t}(\mathbf{d}_{r'}) \times \frac{1 - \beta_{t'}^2}{\eta_{t'}} \left[(1 - \beta_{t'}^2) \overline{K}_t \times U_{r,r',t}^{2,*} - \gamma_{t'}^F (\tau_{r,r',t'} - (\tau_r^B + \tau_{r'}^B)) \right] \geq \mathbf{d}_{r'}$$

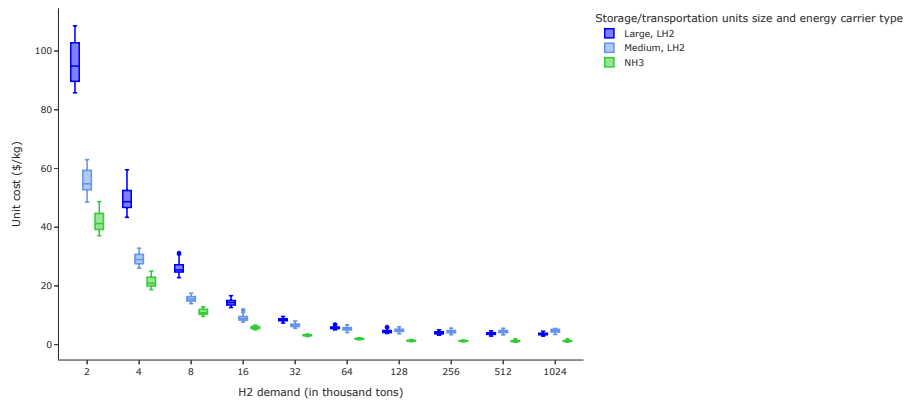
$\chi_{r,r',t}$ is computed under the assumption of a 100 % utilisation rate of transportation capacities and a given optimal number of ships $U_{r,r',t}^{2,*}$, such that $\chi_{r,r',t}$ is a lower bound for the actual number of trips. By construction $\chi_{r,r',t} \times (U_{r,r',t}^{2,*})^{-1}$, equal to the number of trips per year per ship, cannot

exceed a given ceiling, corresponding to the maximum number of trips of a single vessel can complete within a full year. Thus, the required number of ships will evolve by jumps as $\chi_{r,r',t}$ reaches this threshold, such that the "marginal" ship is under-utilized but will allow for economies of scale as its utilization will increase with $\mathbf{d}_{r'}$.

2.2 Unit cost distribution analysis, by energy carrier and technology size



(a) Own cargo propulsion



(b) Conventional marine fuels propulsion

Figure 1: Distribution of transportation unit cost, by energy carrier and technology size

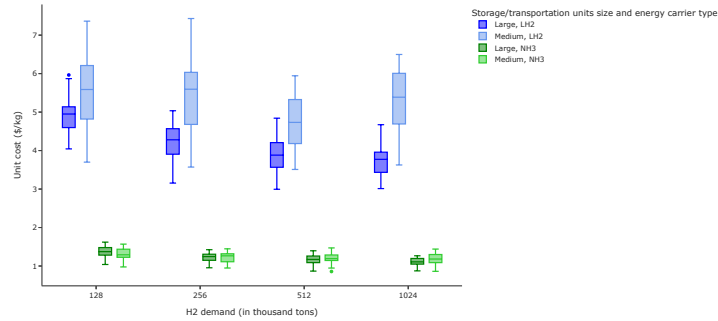
The following key results can be observed from Figure 1 above:

- Unit transportation cost are extremely high for low imported quantities and decrease rapidly. For medium-sized NH3, the unit cost corresponding to 2 kton/year decreases from [36.93-48.43] \$/kg to [0.86-1.44] \$/kg for 1024 kton/year. Unit transportation costs exhibit a stronger reduction for large-sized NH3, decreasing from [41.31-53.99] \$/kg to [0.87-1.27] \$/kg. The average unit cost with large-sized units (resp. medium-sized units) and NH3 carrier falls from 47.12 \$/kg to approximately 1.10 \$/kg (resp. from 42.44 \$/kg to 1.18 \$/kg).

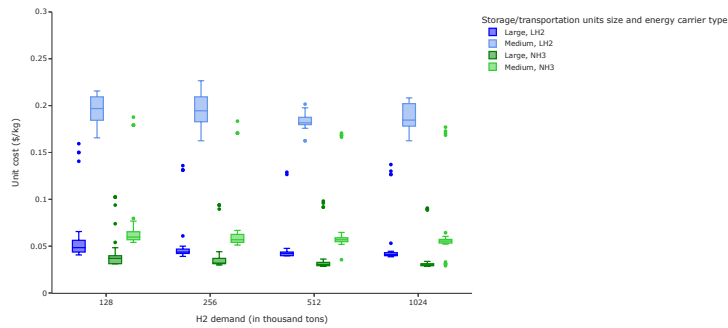
By comparison, the unit transportation cost with medium-sized units and LH2 carrier decreases from [49.52-65.38] \$/kg to [3.62-6.50] \$/kg (resp. from [80.74-104.93] \$/kg to [3.01-4.67] \$/kg for large-sized units). On average, the unit transportation costs for imported quantities above 1024 kton/year are respectively 3.3 and 4.5 times larger for large-sized and medium-sized units compared to NH3 carrier, with values equal to 3.78 \$/kg and 5.27 \$/kg.

- For a technology unit size, there exist significant and robust differences in unit cost distributions between NH3 and LH2 carriers. Because of the non-normality of distributions (significant positive or negative skewness, see below), we use the two-sided Kolmogorov-Smirnov test to compare unit cost distributions between LH2 and NH3 energy carriers. With a p -value above the significance threshold of 0.1 for all import volumes, both when comparing medium-sized and large-sized units, we deduce the cost distributions do not intersect when comparing them across unit size and imported quantity.
- Finally, when comparing across technology sizes for a given energy carrier, the differences in cost distributions between medium-sized and large-sized units are more pronounced for LH2 carrier, with a reversion of the cost hierarchy in favour of large-sized units for important imported quantities. This translates differences in economies of scale dynamics (see Figure 3 below), with distinct convergence speed to steady-state unit cost distributions. A similar but weaker trend can be observed for NH3 energy carrier.

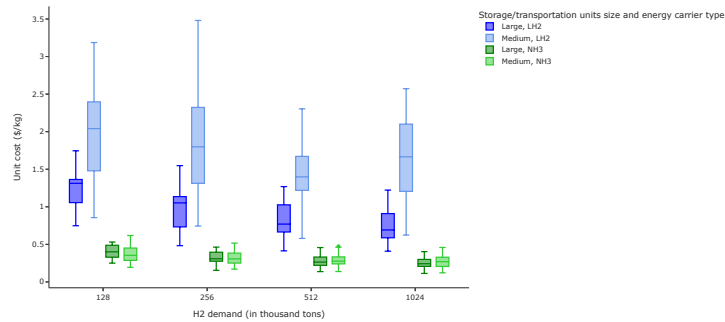
Similar conclusions can be drawn for conventional marine fuels propulsion, with an average unit cost for large-sized units (resp. medium-sized units) for LH2 carrier falling from 96.28 \$/kg to approximately 3.61 \$/kg (resp. from 55.53 \$/kg to 4.61 \$/kg). Although it remains high, the average unit cost corresponding to 1024 kton/year is almost 8 % lower than with cargo-based propulsion for an identical volume. This suggests stronger economies of scale, as confirmed in Figure 3 below.



(a) Full H2 transportation cost



(b) Overseas only H2 transportation cost



(c) DES contract based H2 transportation cost

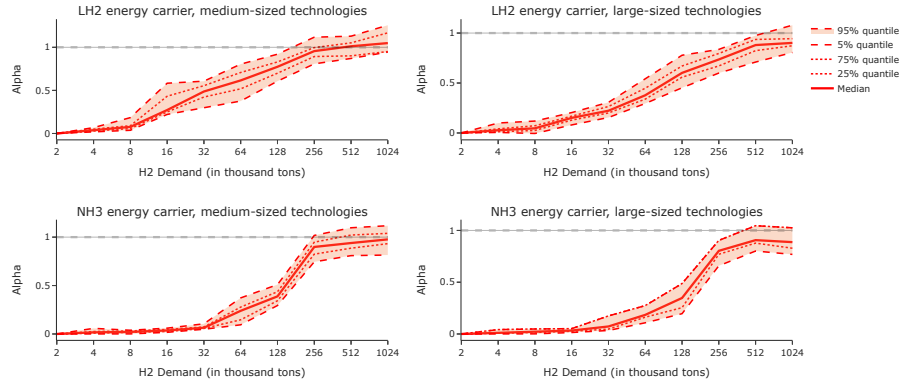
Figure 2: Comparison of the distribution of transportation unit cost, by energy carrier and technology size (own cargo propulsion)

Although we adopted a comprehensive definition of hydrogen transportation cost, including conversion, storage and shipping steps, our decomposition of the total transportation cost by cost categories allows comparisons. In Schuler et

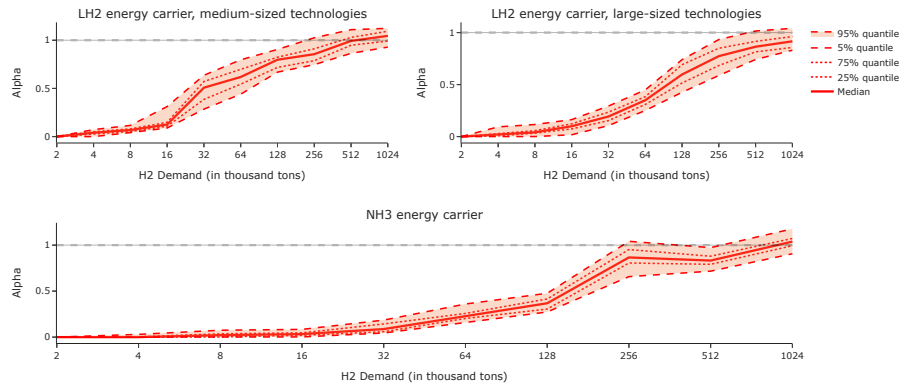
al., 2024, the authors provide a comprehensive and systematized review of shipping cost estimates for various hydrogen-based derivatives, including LH2 and ammonia, across a wide range of international publications. Shipping costs are stated in €/MWh and only include overseas ship costs, thus excluding storage, loading/unloading, conversion and reconversion costs. Using an exchange rate of 0.87 \$/€, corresponding to the 2024 average rate, the estimates for LH2 shipping cost vary between 0.06 \$/kg and 1.86 \$/kg. By comparison, the estimated shipping cost using NH3 as an energy carrier range between 0.01 \$/kg and 0.07 \$/kg. When considering large import quantities (1024 kton/year) , we find in Figure 2.b. that for NH3 with medium-sized and large-sized units the overseas shipping costs are in the intervals [0.03-0.18] \$/kg and [0.03-0.09] \$/kg respectively. Similarly, the shipping cost for LH2 are in the range [0.16-0.63] \$/kg and [0.04-0.14] \$/kg respectively. Our estimates are thus comparable with the values reviewed by Schuler et al., 2024.

Chen et al., 2025 define H2 transportation cost based on the Delivery Ex Ship (DES) contract framework, such that the seller is responsible for delivering the goods at a specified destination port, such that unloading, storage in destination port and reconversion are not considered in the cost evaluation. According to this delivery method, the H2 transportation cost include H2 storage and loading costs in the exporting port, in addition to overseas ship transport costs. Comparing 8 different shipping routes, the authors find levelised unit shipping cost of H2 using NH3 and LH2 energy carriers in the intervals [0.10-0.69] \$/kg and [0.28-1.85] \$/kg respectively. These results are consistent with our findings in Figure 2.c., with corresponding intervals [0.11-0.40] \$/kg and [0.41-1.22] \$/kg for large-sized units.

Our comprehensive definition of hydrogen transportation costs is however justified by the functional dependencies between the successive steps of the hydrogen supply chain. As underlined by Chen et al., 2025, "pricing H2 for end users should consider production, conversion [...], land transport and distribution costs. For example, methanol has the lowest shipping cost in the study, but its higher conversion cost die to higher electricity consumption may offset this advantage". For exporting countries with high electricity costs, the electricity-intensive liquefaction step required when using LH2 carrier significantly increases the total transportation cost. Identical remarks apply to the ammonia cracking step for importing countries. This justifies our comprehensive definition of H2 transportation, as the storage and (re)conversion steps required for transporting H2 under convenient forms cannot be analyzed separately from the overseas shipping step.



(a) Own cargo propulsion



(b) Conventional marine fuels propulsion

Figure 3: Distribution of alpha values, by energy carrier and technology size

As suggested by the rapid decrease in unit costs observed in Figure 1, there exist significant economies of scale for all energy carriers and technology sizes, with import variations across both dimensions. Figure 3 displays the average alpha values for different energy carriers and technology sizes. In terms of interpretation, a value of 0 indicates that doubling the imported quantity does not increase the total transportation cost, such that the unit transportation cost is divided by two. A value of 1 corresponds to increase in total transportation cost exactly equal to the increase in the imported H2 quantity, such that the unit cost is constant.

Three important observations can be made from results:

- First, the magnitude of economies of scale associated to LH2 carrier follows a linear reduction trend for imported quantities above 16 kton/year (especially for medium-sized units), while graphs corresponding to NH3 carrier display a S-shaped curve.
- Second, significant economies of scale are observed for all types of storage/transportation technologies. The strength of economies of scale decreases with imports volume and diseconomies of scale can be observed for values above 256 kton/year for all technological options except large-sized units with LH2 carrier. For instance, the median alpha value for medium-sized NH3 units increases from 0.017 to 0.98, but only exceeds 0.5 (corresponding to a 50 % increase of unit cost following a doubling of imported quantity) for volumes above 128 kton/year. By comparison, the median alpha value for medium-sized LH2 units goes from 0.038 to 1.048, corresponding to strong diseconomies of scale for trade volumes above 256 kton/year for at least 50 % of maritime trade routes.
- Finally, it directly follows from the comparison between energy carrier that transportation logistic chains using NH3 exhibit much stronger economies of scale. Indeed, for medium-sized NH3 units and import quantities inferior or equal to 128 kton/year, roughly 95 % of trade routes exhibit alpha values below 0.5. By comparison, roughly 50 % of routes exhibit values above 0.5 % for import quantities above 32 kton/year for LH2 units. Interestingly, the magnitude of economies of scale converge for large imported quantities, with the same trend observed for large-sized units. Finally, when comparing unit sizes for a given energy carrier, we observe stronger economies of scale for large-sized units, especially for LH2 units. At least 95 % of alpha values below 1 for trade volumes above 512 kton/year for large-sized units (against 50 % with values above for medium-sized ones), which explain the inversion of the cost hierarchy observed in Figure 1. A similar observation can be made when comparing LH2 units by size for logistic chains using ships with conventional marine fuels for propulsion.

Gathering above observations, the MES is reached by only 50 % of (resp. 25 %) of maritime routes using large-sized units (resp. medium-sized units) and NH3 carrier for import quantities equal to 1024 kton/year. A similar conclusion applies to large-sized units with LH2 carrier, while medium-sized ones reach the MES for approximately 50 % of routes beyond 256 kton/year.

At first, one may conclude that significant trade volumes, above 1 million tons/year, are required to reach economic efficiency for most transportation options. However, a closer investigation of Figure 2.a. suggests significantly lower MES values for NH3 carrier: with a unit cost interval of [0.95-1.44] \$/kg for 256 kton/year, the unit cost distribution for medium-sized units is not statistically different from the unit cost distribution corresponding to 1024 kton/year. Indeed, we cannot reject the KS test null hypothesis that samples were drawn

from a unique distributions (p -value = 0.11). This suggests the distribution of unit transportation costs with medium-sized units and NH3 carrier is relatively stable for imported quantities above 256 kton/year. Similarly for large-sized units, the difference between distributions corresponding to 512 kton/year and 1024 kton/year is only statistically significant at the 10 % level. The same conclusions apply with medium-sized and large-sized units and LH2 carrier, for imported quantities above 128 kton/year (p -value = 0.45) and 512 kton/year (p -value = 0.49) respectively.

Our results show logistic hydrogen transportation chains using medium-sized units with either LH2 or NH3 carrier can achieve cost efficiency for relatively low trade volumes. However, following cost and technical assumptions made in this paper, the lowest achievable cost per unit with NH3 carrier remains significantly inferior for all considered trade routes.

2.3 Cost distribution analysis by cost category

In this section, we focus on the cost decomposition of the hydrogen transportation cost and its allocation between exporting and importing regions. Figure 4 to Figure 8 below display the distribution of the shares of each cost category in total transportation cost for CAPEX cost categories, by energy carrier and technology unit size. CAPEX cost categories include conversion and storage CAPEX costs in exporting countries, in addition to reconversion and storage CAPEX costs in importing countries.

In a similar fashion, Figure 9 to Figure 11 exhibit the distribution of shares of each cost category in total transportation cost for OPEX cost categories. These include conversion technologies variable OPEX costs in origin and destination countries respectively, in addition to variable transportation costs (canal and port charges). To avoid an overwhelming number of figures, the results displayed in this report are computed for ships using their own cargo for propulsion only. Thus, CO2 emission costs and fuel cost, associated to ships consuming conventional marine fuels, are not included here. Finally, storage variable costs are negligible and are thus not displayed.

Regarding the general results that can be drawn, we observed that the shares of CAPEX costs globally decrease with import volumes, with initial divergences between unit sizes for a given energy carrier eventually decreasing with the magnitude of hydrogen trade. The inverse tendency is observed for OPEX costs: their shares increase with import volumes, as well as the discrepancies between the distributions with medium-sized and large-sized units.

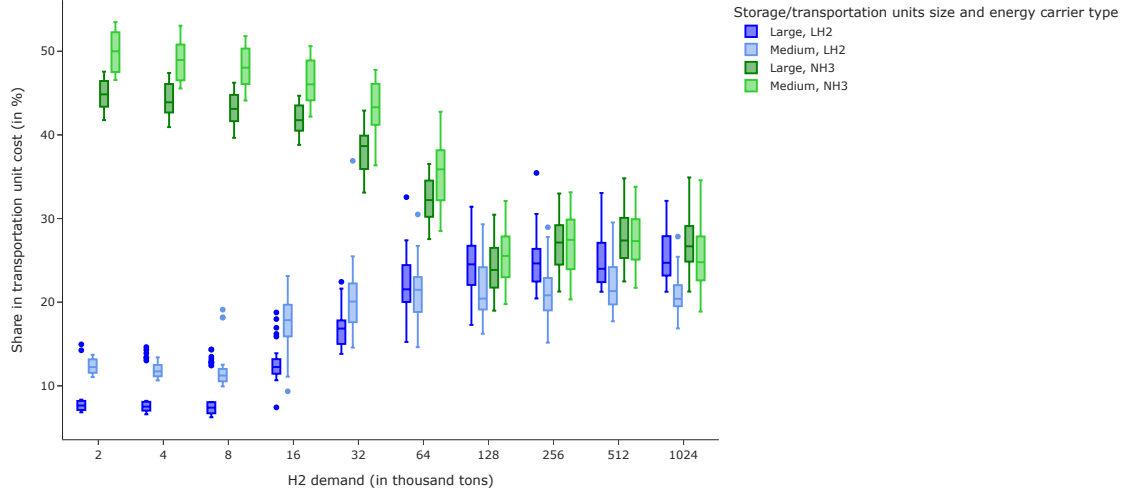


Figure 4: Distribution of the share in total costs of conversion technology units CAPEX in exporting countries, by energy carrier and technology size

As observed in Figure 4, the shares of conversion CAPEX cost are significantly larger when investing in Haber-Bosch units than in liquefaction units for imported quantities below 128 kton/year and all unit sizes. The four distributions converge for large trade volumes, with a sustained gap between LH2 transportation logistic chains with medium-sized and large-sized units however. The average share of conversion CAPEX costs with large-sized units (resp. medium-sized units) with NH3 energy carrier decreases from 44.9 % (resp. 49.9 %) to 26.9 % (resp. 25.3 %). By comparison, the average shares associated with large-sized units and LH2 energy carrier increase from 7.91 % to 25.8 %.

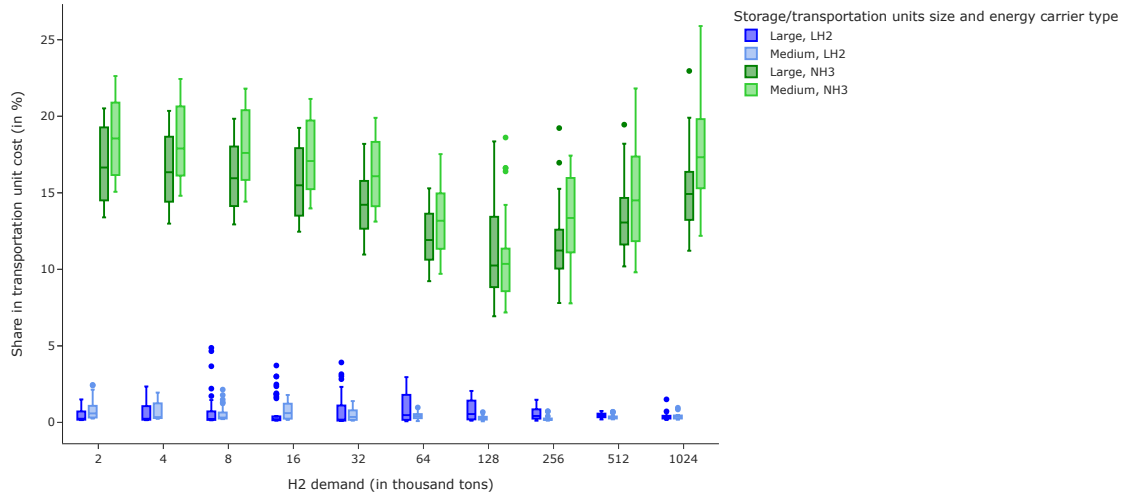


Figure 5: Distribution of the share in total costs of conversion technology units CAPEX in importing countries, by energy carrier and technology size

Interestingly, Figure 5 above shows that the shares of reconversion CAPEX costs is relatively insensitive to the volume of imports. Indeed, when considering large-sized units and NH3 energy carrier, the shares vary from [13.39-20.51] % for 2 kton/year to [11.21-19.91] % for 1024 kton/year, with corresponding average values between 16.8 % and 15.1 %. Similar conclusions apply to medium-sized units, with slightly higher shares for the majority of trade routes. Because of the very low CAPEX cost of regasification units associated to LH2 energy carrier, their average share for medium-sized and large-sized units remains below 1 %. These results may however be associated to the absence of constraints on the dynamics of hydrogen consumption in import countries, which may smooth the withdrawal profile from storage units and thus underestimate regasification needs for peak demand periods.

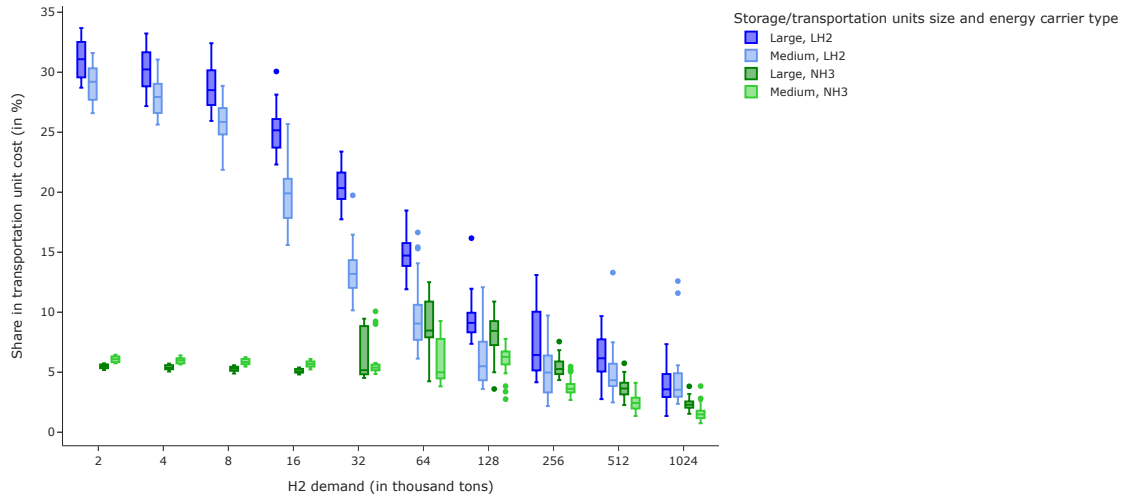


Figure 6: Distribution of the share in total costs of storage technology units CAPEX in exporting countries, by energy carrier and technology size

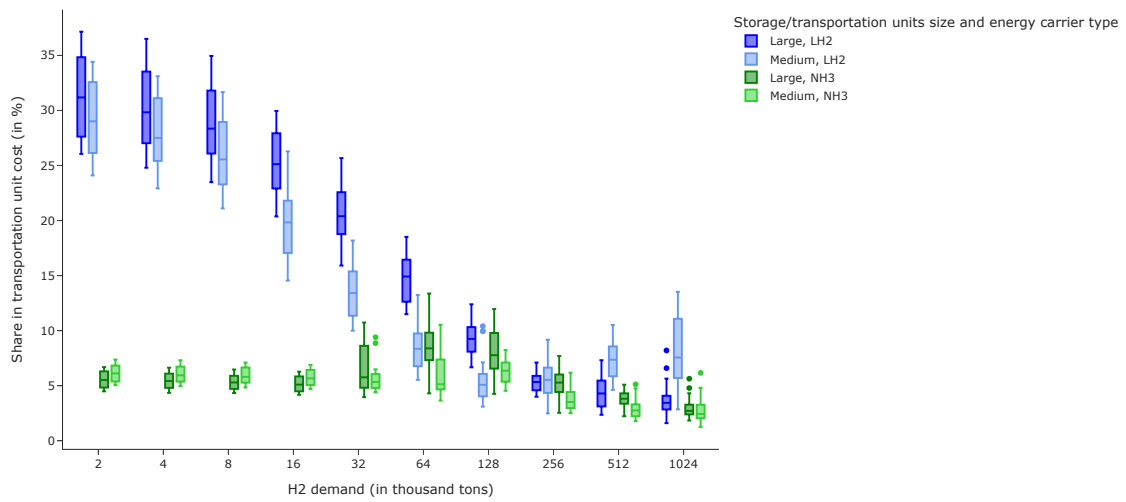


Figure 7: Distribution of the share in total costs of storage technology units CAPEX in importing countries, by energy carrier and technology size

Figure 6 and Figure 7 indicate similar patterns for the evolution of shares

associated to storage units CAPEX in exporting and importing countries. The shares associated to NH3 are globally independent from imported quantities and similar across unit sizes. For exporting regions (resp. importing regions), the shares associated to medium-sized units range from [5.74-6.41] % to [0.74-2.62] % (resp. [5.04-7.37] % to [1.25-4.81] %) across all imported quantities. The much higher shares associated to LH2 energy carrier are a direct consequence of the significantly larger CAPEX cost of LH2 storage tanks. Finally, we note that the divergences and larger variance observed for intermediate import volumes (between 32 and 128 kton/year) may be created by thresholds associated to the saturation of existing storage units, which depend on the storage pattern and distance between the pair of countries considered.

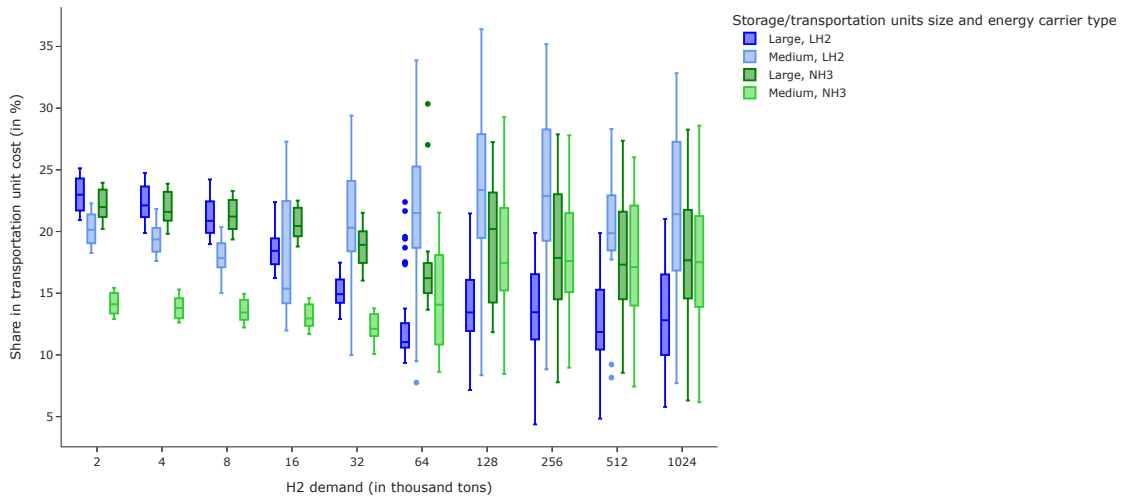


Figure 8: Distribution of the share in total costs of transportation technology units CAPEX, by energy carrier and technology size

Finally, Figure 8 displays a quite unclear picture of the shares of transportation unit CAPEX in total cost. For small import volumes, the discrepancies between the distributions clearly reflect the differences in CAPEX costs between the available transportation technologies, and correspond to a situation where a single vessel is sufficient. However, the variance of the shares strongly increase for import volumes above 128 kton/year, such that it is not possible to identify statistically significant difference between distributions across carrier type and unit size. This suggests the share of transportation unit CAPEX is highly sensitive to country specific exogenous parameters and more importantly maritime distance.

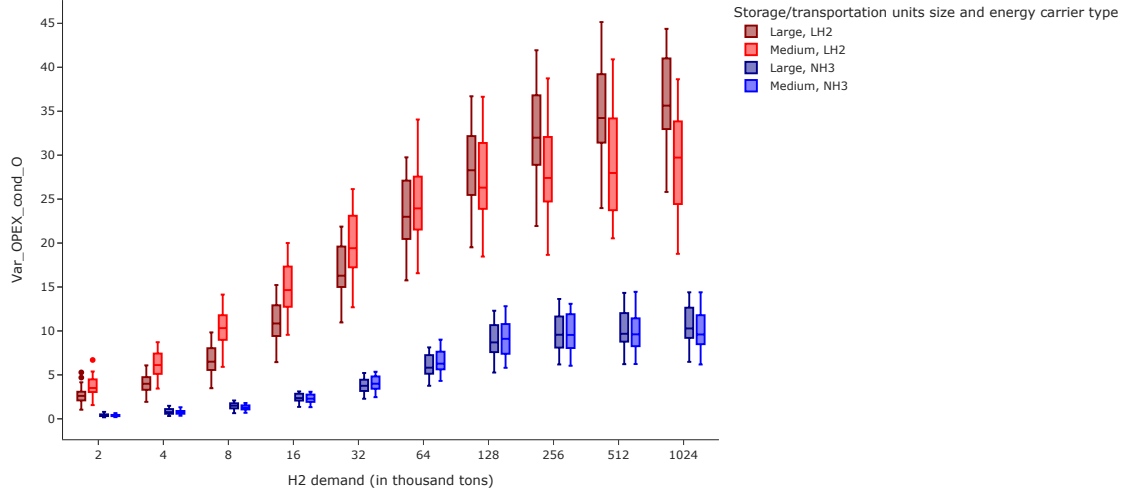


Figure 9: Distribution of the share in total costs of conversion technology units OPEX costs in exporting countries, by energy carrier and technology size

Not surprisingly, Figure 9 displays very high shares of variable OPEX costs associated to liquefaction. Indeed, with large-sized (resp. medium-sized) units, the shares increase from [1.03-4.16] % for 2 kton/year to [25.81-44.38] for 1024 kton/year % (resp. [1.56-5.39] % to [18.77- 38.64] %). This indicates that for a 'mature' transportation logistic chain corresponding to large import volumes, liquefaction cost require roughly one third of the total transportation cost. By comparison, although the share of OPEX costs associated to Haber-Bosch conversion units increase with the volume of imports, its values remaining in the interval [5.26-14.45] % for volumes beyond 128 kton/year and all unit sizes.

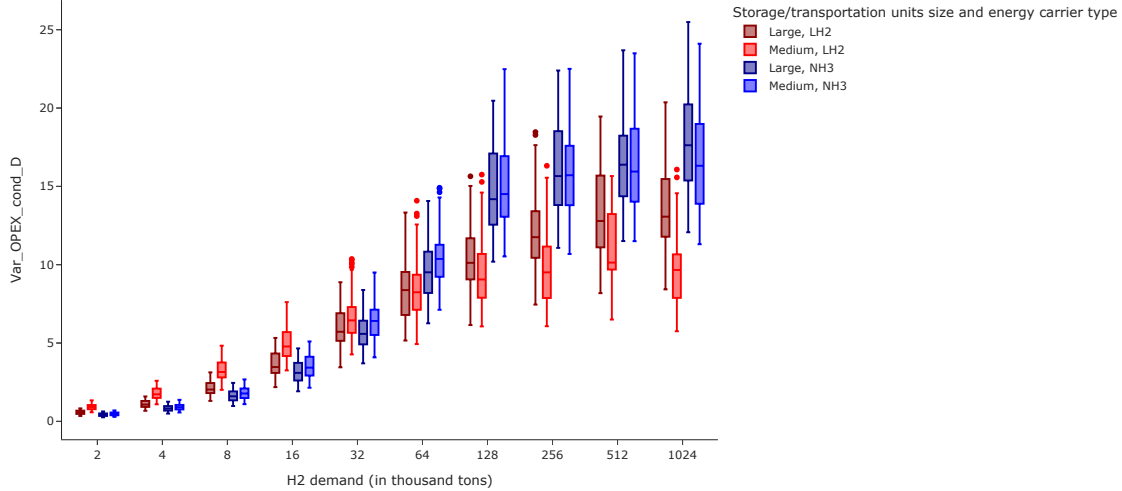


Figure 10: Distribution of the share in total costs of conversion technology units OPEX costs in importing countries, by energy carrier and technology size

Interestingly, Figure 10 displays a similar pattern but with an inversion of the cost hierarchy between the LH2 and NH3 transportation logistic chains. For import volumes between 128 kton/year and 1024 kton/year, the shares of ammonia cracking costs with large-sized (resp. medium-sized units) range from [10.19-20.46] % to [12.07-25.49] % (resp. [10.52-22.48] % to [11.30-24.11] %). For the same trade volumes, regasification variable costs account for approximately 10 to 13.5 % of total transportation costs on average with large-sized units.

Keeping in mind that the variable costs of liquefaction, regasification, conversion and ammonia cracking are uniquely composed of electricity costs by assumption, our results indicate that for a 'mature' logistic chain with large import volumes, more than 40 % of the total transportation cost would be directly submitted to electricity price fluctuations on average. The important economies of scale achieved by large-sized units are thus partially offset by an increasing power price risk, which requires long-term electricity procurement contracts to hedge against price volatility in both exporting and importing regions. A careful investigation of the utilization rates of each type of technology would be fruitful to better understand the interaction of operational constraints and decisions with investment decisions. Although utilization rates can directly be computed from our results, we leave this research topic open for further work.

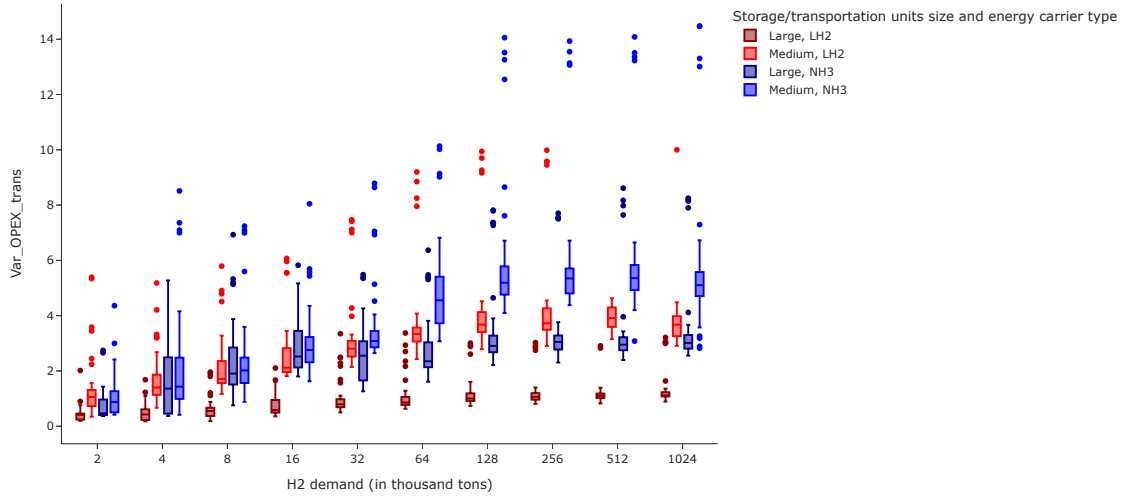


Figure 11: Distribution of the share in total costs of transportation technology units OPEX costs, by energy carrier and technology size

Finally, Figure 11 displays a pattern corresponding exactly to the inverse of Figure 8. For very low import volumes, a single round-trip may be sufficient to satisfy demand in importing countries, such that differences in capacity between transportation technologies are irrelevant. However, for large import volumes, large-sized transportation units require significantly less trips than medium-sized ones, which translates into lower transportation variable costs.

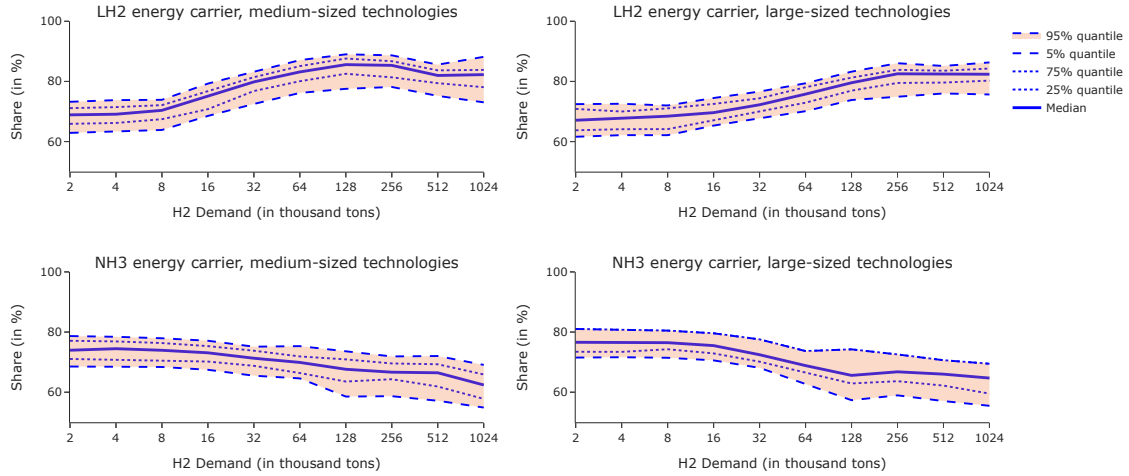


Figure 12: Distribution of the shares of exporting regions in total costs of transportation, by energy carrier and technology size

Figure 12 provides a different perspective on the distribution of transportation costs, by investigating their allocation between exporting and importing regions. We assume the share of exporting countries in total transportation costs includes conversion, storage in exporting port and shipping costs. We observe opposite trends for LH2 and NH3 carriers: the share of exporting countries increases with imported quantities for the former, while it decreases for the latter. For medium-sized units (resp. large-sized units) transporting quantities above 128 kton/year with LH2 energy carrier, exporting countries bear at least 73 % (resp. 75 %) of all transportation costs for 95 % of trade routes. While the majority of costs are still borne by exporting regions with NH3 carrier, their share with medium-sized units (resp. large-sized units) range from [58.54-73.60] % for 128 kton/year to [58.90-69.08] % for 1024 kton/year (resp. [57.34-74.25] % to [55.48-69.45] %). These dynamics can be directly related to the initially high share of Haber-Bosch conversion units for NH3 carrier, and the increasing share of liquefaction electricity costs for LH2 carrier. For all technological options, we still note that between 70 % and 80 % of costs are borne by exporting regions for small import volumes, such that most of the investment risk is supported by exporters. This justifies the elaboration of cooperative strategies and risk-sharing agreements between exporting and importing regions, especially in the early-stages of the hydrogen transportation chain.

2.4 Total cost analysis

Although the production and transportation costs of hydrogen are determined independently, the latter influences the choice of the optimal transportation logistic chain.

To better understand this point, let us define $\lambda_{r,r',t}(\mathbf{X}_{r,r',t}^*) \triangleq \lambda_{r,r',t}(\mathbf{X}^*)$ as the ratio between the net imported volume in region r' and shipped with transportation technology $t \in \mathcal{T}_T$, and the volume of gaseous hydrogen initially produced in region r . Furthermore, $\mathbf{X}_{r,r',t}^*$ is optimal total number of trips for $t \in \mathcal{T}_T$ between region r to r' . Formally, we define $\lambda_{r,r',t}(\mathbf{X}^*)$ as follows:

$$\lambda_{r,r',t}(\mathbf{X}^*) = \mathbf{d}_{r'}^{-1} \times \left[\left(\mathbf{d}_{r'} \times \left(\sum_{p' \in \mathcal{P}(t)} \frac{1}{\eta_{p',p}(1-\beta_t^2)} \right)^{-1} + \gamma_t^F (\tau_{r,r',t} - (\tau_r^B + \tau_{r'}^B)) \mathbf{X}_{r,r',t}^* \right) \times \left(\sum_{p' \in \mathcal{P}(t)} \frac{1}{\eta_{p',p}(1-\beta_t^2)} \right)^{-1} \right]$$

In terms of interpretation, the above equation indicates that in order to import a net volume equal to $\mathbf{d}_{r'}$ ktons/year of gaseous hydrogen in region r' , it is required to produce $\lambda_{r,r',t}(\mathbf{X}^*) \times \mathbf{d}_{r'}$ ktons in region r .

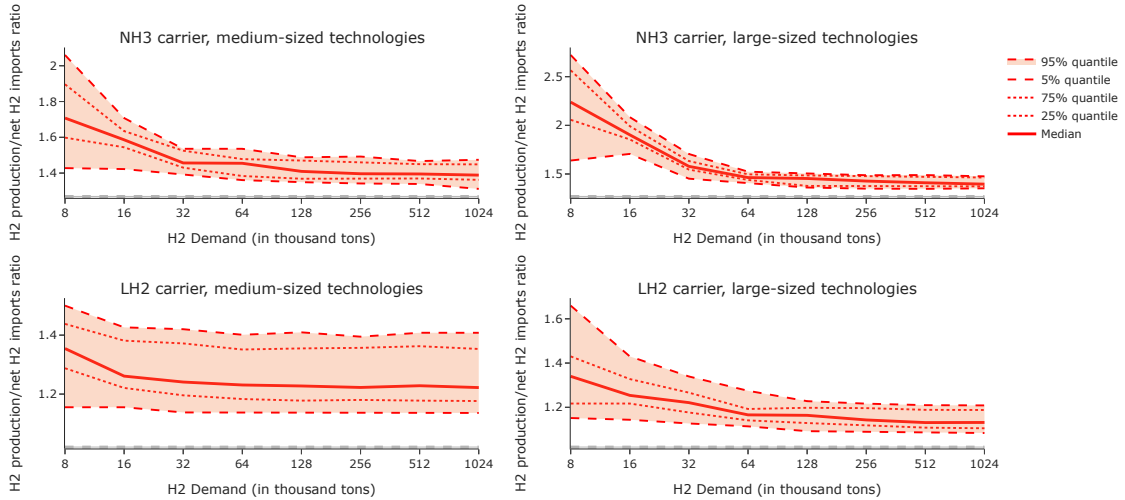


Figure 13: Distribution of H2 production to net H2 imports ratios, by energy carrier and technology size

Figure 13 displays the distribution of $\lambda_{r,r',t}(\mathbf{X}^*)$ for transportation technologies using their own cargo for propulsion. The gray lines correspond to

the values associated to transportation technologies using marine fuels, which is constant as it is independent of $\mathbf{X}_{r,r',t}^*$.

While initially higher, the distributions of ratios for NH3 carrier with large-sized converge to the distribution corresponding to medium-sized units for imported quantities above 64 kton/year. For large-sized units, the use of NH3 carrier requires for 90 % of trade routes the production of approximately [1.36-1.50] times the mass of delivered hydrogen for net imported quantities above 128 kton/year. Medium-sized units exhibit very similar results. Put differently, this suggests that for a net imported quantity of 1024 kton/year, it is necessary to produce roughly between 1390 kton/year and 1535 kton/year of gaseous hydrogen to satisfy demand. By comparison, the distribution of the ratio of produced to distributed hydrogen is remarkably stable when using LH2 carrier. For traded quantities above 128 kton/year, it ranges for 90 % of routes in the intervals [1.14-1.41] and [1.09-1.22], for medium-sized and large-sized units respectively. These significant differences between LH2 and NH3 correspond to the conversion and reconversion losses between gaseous hydrogen and ammonia required for storage and shipping.

We can finally use the above results to compute the total unit cost of imported hydrogen, which takes into account the extra production cost of hydrogen lost in the conversion, storage and shipping processes. By noting P_r the production cost of hydrogen in region r , expressed in \$/kg, the total unit cost associated to the satisfaction of annual demand $\mathbf{d}_{r'}$ with imports from region r is equal to $\mathbb{P}_{r,r',t}$:

$$\mathbb{P}_{r,r',t} = P_r \times \lambda_{r,r',t}(\mathbf{d}_{r'}, \mathbf{X}^*) + \mathbf{C}_{r,r'}^*$$

$$, \text{ where } \mathbf{C}_{r,r'}^* = C_r^{1*} + C_{r'}^{1*} + C_r^{2*} + C_{r'}^{2*} + C_{r,r'}^{3*} + C_{r,r'}^{4*}.$$

As expected, our results highlight a robust transportation cost difference in favour of NH3 carrier, even for high hydrogen production cost in exporting regions:

- Indeed, for all technology unit size and imported quantities, the difference between the total unit transportation cost associated to NH3 and LH2 carriers is negative (except for a few outliers), which indicates NH3 is systematically cheaper as an energy carrier for hydrogen transportation. Even for a hydrogen production cost of 4 \$/kg, the unit transportation cost with medium-sized units and NH3 is at least 1.41 \$/kg lower for all trade routes and imported quantities above 16 kton/year (see Figure 14). The same conclusion applied to vessels using conventional marine fuels for propulsion: the total hydrogen unit cost associated to NH3 carrier is consistently lower for all routes and traded quantities.

- For large-sized units however (see Figure 15), the cost differential significantly decreases with traded quantities but remains consistently negative. This suggests LH2 could however compare favorably to NH3 for very high hydrogen production costs and traded quantities, assuming reduction in CAPEX costs for LH2 conversion, storage and transportation units. The cost difference may also be economically acceptable for end-uses requiring high purity hydrogen, which favours LH2 transportation solutions. Note that the cost of purification is not included in our modeling. Yet, even for a high hydrogen production cost of 4 \$/kg (resp. 6 \$/kg), the total unit cost with NH3 remains 1.03 \$/kg (resp. 0.51 \$/kg) lower for 1024 kton/year in 95 % of cases. Except for capacity and resources constrained countries, the total cost of imported hydrogen is likely to be higher than the cost of domestic production in this specific case.

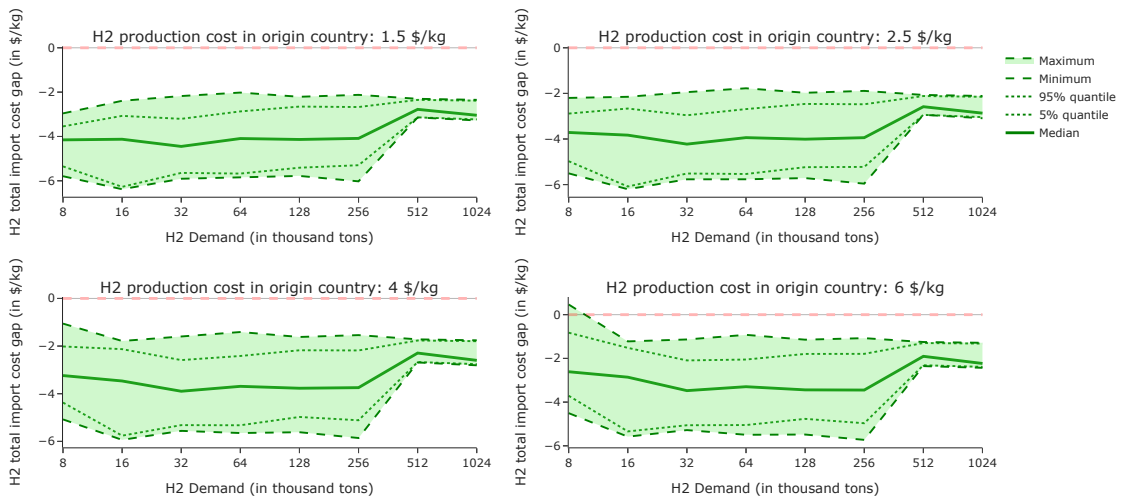


Figure 14: H2 total unit cost difference (LCOH + LCOT) between NH3 and LH2 energy carriers, with medium-sized technologies

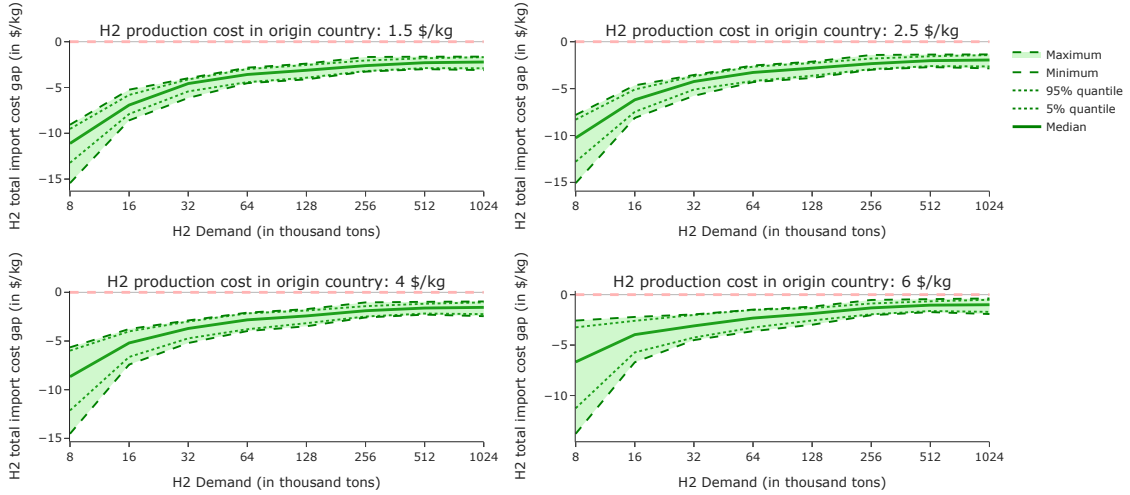


Figure 15: H2 total unit cost difference (LCOH + LCOT) between NH3 and LH2 energy carriers, with large-sized technologies

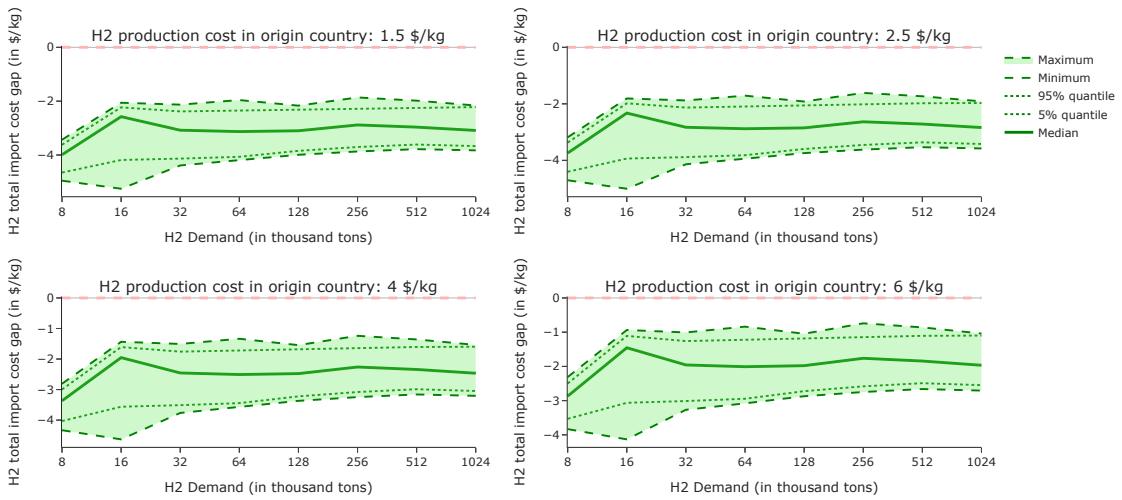


Figure 16: H2 total unit cost difference (LCOH + LCOT) between NH3 and LH2 energy carriers (conventional marine fuels propulsion)

As a general conclusion of the above analysis, our results provide robust evidence that NH₃ carrier is the optimal solution on the basis of total transportation costs. Following Erdemir and Dincer, 2024, NH₃ transportation offers several key advantages for a quick transition to the hydrogen economy. Indeed, green ammonia transportation benefits from existing infrastructures for production, storage and shipping that can be leveraged, in addition to existing safety standards and regulations. Finally, the logistics and supply chain for ammonia production and transportation are already mature and well-established, with large quantities transported worldwide.

The above results however provide a statistical analysis of the behaviour of hydrogen transportation costs, for a wide variety of maritime routes. Using our simulation results as our training set, the final subsection of this paper uses simple econometric tools to get an overview of the influence of exogenous factors, including distance, electricity prices and WACC, on route-specific transportation costs.

2.5 Econometric insights of exogenous factors influencing H₂ transportation cost

As discussed in Chen et al., 2025, various factors influence H₂ shipping costs, including maritime distance, ship capacity, storage capacity, ship fuel consumption, BOG intensity, storage losses and carbon tax. However, most of the above factors are a direct consequence of a specific or storage vessel design, which we cannot vary except by comparing transportation chains with medium-sized and large-sized units. In the following econometric analysis, a separate regression is thus conducted for each combination of energy carrier and technology size. Our set of exogenous variables include maritime distance, net imported quantity, exporting/importing country WACC and exporting/importing grid electricity price.

For each couple of regions, we investigate the individual effects of exogenous parameters of the total transportation cost. We use the total transportation instead of unit transportation cost to avoid non-linearities introduced by the scaling of the total cost by net imported quantity. We also use the transportation cost as defined by DES contracts for the sake of comparison. We expect strong interaction effects between exogenous variables, as for a given technological option, their respective impacts vary with the share of each cost category in the total transportation cost. For each combination of energy carrier and technology size, we thus perform two separate OLS linear regression, with and without interaction effects. To facilitate interpretation, both the dependent and independent variables are standardized, such that regression coefficients measure the correlation between the independent and dependent variables, which makes their magnitudes comparable.

Regression tables and results are provided in the Appendix. As expected,

the imported quantity and the maritime distance have the largest influence on total transportation cost. For large-sized units (resp. medium-sized units) and LH2 carrier, the corresponding OLS regression coefficients in Table 7 are 0.992 and 0.060 (resp. 0.988 and 0.084), both significant at the 1 % level. With a standard deviation of 4945 km, this implies a 1000 km increase in maritime distance causes on average a 4 257 million \$ increase in total cost. This result (approximately 4 \$/kg/1000 km increase for 1024 kton/year) is incompatible with small spread of the unit cost distribution found in Figure 1. This justifies the use of interaction terms to capture the interplay between imported quantity and distance. As foreshadowed, the coefficient corresponding to their interaction is large (0.233 and 0.320 with large-sized and medium-sized units respectively) and strongly significant. The interaction of imported quantity and electricity cost in exporting region is also quite large (0.163 and 0.102), which captures the growing weight of liquefaction costs as the volume of trade increases. Unsurprisingly, the magnitude of the coefficients associated to distance when using transportation cost based on the DES contract framework is significantly higher (see Table 9): it reaches 0.184 and 0.177 with large-sized and medium-sized units respectively. However, the negative signs associated to the coefficients for the interaction of distance and electricity costs suggests our specification is incorrect.

Identical conclusions apply to the case of NH3 carrier, with lower magnitudes for the coefficients associated to import volume, distance and their interaction however (see Table 6 and Table 8). Coefficients associated to the WACC in exporting and importing regions are also higher, which highlights the importance of higher upfront investment costs when using NH3 carrier. Overall, our findings are consistent with those of Perey and Mulder, 2023, with ammonia transportation being less sensitive to distance and lower shipping costs per distance unit.

The presence of non-linearities in our investment and operational model however limits the quality of a linear approximation of total transportation costs. Figure 17-18 in Appendix display the relative OLS regressions prediction errors with NH3 and LH2 carrier, with lighter colors corresponding to larger quantities of imported hydrogen. We note the presence of both prediction bias (corresponding to the red line, obtained by applying Gaussian process regression on residuals) and heteroscedasticity. Both the bias and variance decrease with the imported quantity, which suggests a linear regression better predicts total transportation costs for large trade volumes. Adding interaction effects reduces the variance of errors and bias but does not solve the heteroscedasticity issue. These insights suggests more intricate specifications, like Generalized Additive Models (GAMs) or regression trees, may be required when constructing a surrogate model for the behaviour of hydrogen transportation costs. We leave these questions open for further research.

3 Conclusions

The analysis of the results for our case study covering several countries indicates that, in terms of international maritime trade of low-carbon hydrogen, significant economies of scale are achievable for all energy carriers and all storage/transportation unit sizes. These economies of scale can be obtained across different transport logistics chains (in our case, NH₃ and LH₂), but, depending on the evolution of demand, they would have a lesser impact on the marginal transport cost for ammonia-based energy carriers (NH₃) than for LH₂, even though the transport cost of LH₂ remains higher compared to that of NH₃. The unit cost of hydrogen transportation using NH₃ as a carrier is consistently lower than the cost associated to LH₂, for all selected technology sizes and maritime routes.

The analysis of the results also indicates that diseconomies of scale can be observed, as is the case for medium-sized LH₂ units for large volumes of demand. For exporters, the average share of investment costs related to conversion for large-scale (and medium-scale) units using ammonia as an energy carrier decreases by almost half. In comparison, the average share associated with large-scale units and liquid hydrogen as an energy carrier increases from 7.4% to 24.9%. For importers, the results indicate that the share of investment costs related to conversion is relatively insensitive to the volume of imports. Nevertheless, the results also indicate that the share of capital expenditures of transport units is highly sensitive to country-specific exogenous parameters and, above all, to the sea distance. For LH₂, the analysis of the distribution of each cost category shows very significant shares for the operating costs of the liquefaction units, and that for large import volumes, liquefaction costs represent approximately one-third of the total transport cost. By comparison, although the share of operating costs associated with the Haber-Bosch conversion units increases with the volume of imports, its average value remains between 10% and 11% for volumes exceeding 128 kt/year.

However, our model compares the two options on the sole basis of total transportation costs. As underlined by Boissonnet and Popiolek, 2024, several criteria must be considered for a comprehensive comparison, including R&D risk, technological maturity, environmental and health safety, climate risk or navigation safety. Studying the case of hydrogen shipping from Australia to Japan, the authors provide a multicriteria analysis, with different rankings between LH₂, NH₃ and LOHC depending on the weight attributed to each criterion.

Our results provide a robust and comprehensive quantitative basis for further analysis of investment decisions and coordination issues relative to the early-stages of an international hydrogen supply chain, in particular when risk aversion and cost uncertainties are considered. These specific research questions will thus be investigated in future work.

4 Appendix

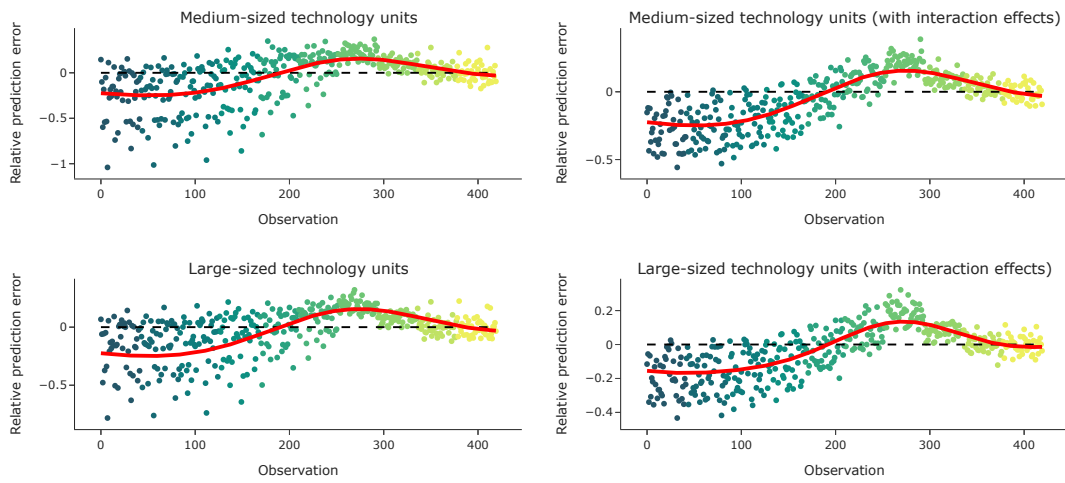


Figure 17: Relative linear regression prediction error with NH₃ energy carrier

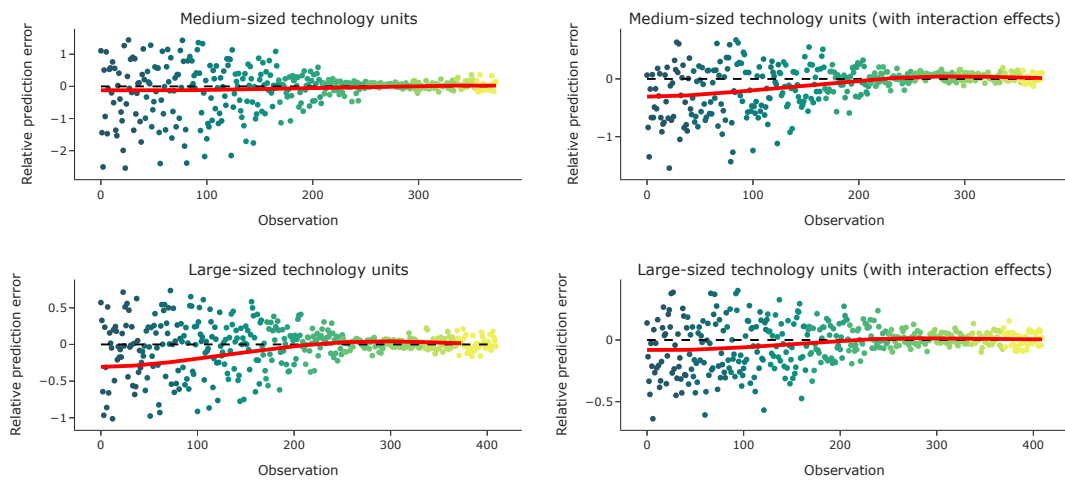


Figure 18: Relative linear regression prediction error with LH₂ energy carrier

Origin/Destination	Australia	Brazil	South-Africa	United-States	China	Morocco
France	19.809	9.543	11.677	9.233	18.772	2.141
Australia		14.822	10.950	17.857	8.665	18.689
Brazil			6.946	11.221	20.607	7.780
South-Africa				15.446	13.780	9.939
United-States					18.102	8.957
China						17.652

Table 4: Average maritime distances between selected countries [in thousand kilometers]

Country	Electricity price [in k\$/MWh]	CO2 price [in k\$/ton]
France	0.135	0.047
Australia	0.134	0.052
Brazil	0.108	0
South-Africa	0.169	0.009
United-States	0.106	0
China	0.109	0.008
Morocco	0.083	0

Table 5: Average electricity price and CO2 price in selected countries

	NH3			
	Medium	Large	Medium	Large
Import volume	0.989 ^{***}	0.991 ^{***}	0.651 ^{***}	0.695 ^{***}
Distance	0.062 ^{***}	0.056 ^{***}	0.017	0.026
WACC _{<i>t</i>}	0.044 ^{***}	0.054 ^{***}	0.044 ^{***}	0.046 ^{***}
WACC _{<i>t'</i>}	0.009	0.014 ^{**}	0.023	0.024 [*]
Electricity cost _{<i>t</i>}	0.019 ^{***}	0.015 ^{***}	0.005	0.015
Electricity cost _{<i>t'</i>}	0.029 ^{***}	0.029 ^{***}	0.013	0.015
Import volume × Distance			0.249 ^{***}	0.190 ^{***}
Import volume × WACC _{<i>t</i>}			0.049 ^{***}	0.101 ^{***}
Import volume × WACC _{<i>t'</i>}			0	0
Import volume × Electricity cost _{<i>t</i>}			0.009	-0.028
Import volume × Electricity cost _{<i>t'</i>}			0.062 ^{***}	0.057 ^{***}
Distance × WACC _{<i>t</i>}			-0.011	-0.001
Distance × WACC _{<i>t'</i>}			-0.037	0.027
Distance × Electricity cost _{<i>t</i>}			0.027	0.006
Distance × Electricity cost _{<i>t'</i>}			0.017	0.011
Number of observations	420	420	420	420
Interaction terms	No	No	Yes	Yes
R^2	0.982	0.988	0.991	0.993
Prob (F-statistics)	0.000	0.000	0.000	0.000
Breusch-Pagan test (p -value)	0.000	0.000	0.000	0.000

t statistics in parentheses

* $p < 0.10$, ** $p < 0.05$, *** $p < 0.01$

Note: Robust standard errors in parentheses

Table 6: Regression table - NH3 carrier

	LH2			
	Medium	Large	Medium	Large
Import volume	0.988 ^{***}	0.992 ^{***}	0.610 ^{***}	0.634 ^{***}
Distance	0.084 ^{***}	0.060 ^{***}	0.021	0.043
WACC _{<i>r</i>}	0.039 ^{***}	0.039 ^{***}	0.041 ^{**}	0.039 ^{***}
WACC _{<i>r</i>'}	0.003	0.006	-0.001	0.015
Electricity cost _{<i>r</i>}	0.045 ^{***}	0.045 ^{***}	0.028	0.023 [*]
Electricity cost _{<i>r</i>'}	0.012	0.016 ^{**}	0.024	0.025 [*]
Import volume × Distance			0.320 ^{***}	0.233 ^{***}
Import volume × WACC _{<i>r</i>}			0.180 ^{***}	0.095 ^{***}
Import volume × WACC _{<i>r</i>'}			0	0
Import volume × Electricity cost _{<i>r</i>}			0.102 ^{***}	0.163 ^{***}
Import volume × Electricity cost _{<i>r</i>'}			-0.188 ^{***}	-0.102 ^{***}
Distance × WACC _{<i>r</i>}			-0.032	-0.018
Distance × WACC _{<i>r</i>'}			0.018	-0.026
Distance × Electricity cost _{<i>r</i>}			-0.002	0.003
Distance × Electricity cost _{<i>r</i>'}			0.015	0.008
Number of observations	374	374	374	374
Interaction terms	No	No	Yes	Yes
R^2	0.973	0.985	0.992	0.994
Prob (F-statistics)	0.000	0.000	0.000	0.000
Breusch-Pagan test (p -value)	0.000	0.000	0.000	0.000

t statistics in parentheses

* $p < 0.10$, ** $p < 0.05$, *** $p < 0.01$

Note: Robust standard errors in parentheses

Table 7: Regression table - LH2 carrier

	NH3 - Comparison with Chen et al. (2025)			
	Medium	Large	Medium	Large
Import volume	0.933 ^{***}	0.939 ^{***}	0.664 ^{***}	0.756 ^{***}
Distance	0.178 ^{***}	0.182 ^{***}	0.056	0.091
WACC _{<i>t</i>}	0.055 ^{***}	0.093 ^{***}	0.094 ^{***}	0.111 ^{***}
WACC _{<i>t'</i>}	-0.026	-0.009	-0.029	0.031
Electricity cost _{<i>t</i>}	0.010	0	-0.014	0.024
Electricity cost _{<i>t'</i>}	0.010	0.002	-0.017	-0.001
Import volume × Distance			0.759 ^{***}	0.739 ^{***}
Import volume × WACC _{<i>t</i>}			0.069 ^{**}	0.038
Import volume × WACC _{<i>t'</i>}			0	0
Import volume × Electricity cost _{<i>t</i>}			-0.199 ^{***}	-0.296 ^{***}
Import volume × Electricity cost _{<i>t'</i>}			-0.157 ^{***}	-0.239 ^{***}
Distance × WACC _{<i>t</i>}			-0.080	-0.052
Distance × WACC _{<i>t'</i>}			-0.141 [*]	-0.108 [*]
Distance × Electricity cost _{<i>t</i>}			0.104 [*]	0.029
Distance × Electricity cost _{<i>t'</i>}			0.099 [*]	0.072
Number of observations	420	420	420	420
Interaction terms	No	No	Yes	Yes
R^2	0.903	0.916	0.971	0.978
Prob (F-statistics)	0.000	0.000	0.000	0.000
Breusch-Pagan test (p -value)	0.000	0.000	0.000	0.000

t statistics in parentheses

* $p < 0.10$, ** $p < 0.05$, *** $p < 0.01$

Note: Robust standard errors in parentheses

Table 8: Regression table - NH3 carrier and DES contract transportation cost

	LH2 - Comparison with Chen et al. (2025)			
	Medium	Large	Medium	Large
Import volume	0.945 ^{***}	0.934 ^{***}	0.780 ^{***}	0.914 ^{***}
Distance	0.177 ^{***}	0.184 ^{***}	0.0170	0.126
WACC _{<i>r</i>}	0.057 ^{***}	0.092 ^{***}	0.093 ^{***}	0.115 ^{***}
WACC _{<i>r</i>'}	-0.057	-0.001	0.007	0.040
Electricity cost _{<i>r</i>}	0.014	-0.004	0.022	0.036
Electricity cost _{<i>r</i>'}	-0.004	-0.014	0.004	0.003
Import volume × Distance			0.752 ^{***}	0.775 ^{***}
Import volume × WACC _{<i>r</i>}			0.051	-0.012
Import volume × WACC _{<i>r</i>'}			0	0
Import volume × Electricity cost _{<i>r</i>}			-0.212 ^{***}	-0.320 ^{***}
Import volume × Electricity cost _{<i>r</i>'}			-0.376 ^{***}	-0.368 ^{***}
Distance × WACC _{<i>r</i>}			-0.086	-0.049
Distance × WACC _{<i>r</i>'}			-0.024	-0.114
Distance × Electricity cost _{<i>r</i>}			-0.016	-0.006
Distance × Electricity cost _{<i>r</i>'}			0.060	0.066
Number of observations	374	374	374	374
Interaction terms	No	No	Yes	Yes
R^2	0.894	0.898	0.977	0.972
Prob (F-statistics)	0.000	0.000	0.000	0.000
Breusch-Pagan test (p -value)	0.000	0.000	0.000	0.000

t statistics in parentheses

* $p < 0.10$, ** $p < 0.05$, *** $p < 0.01$

Note: Robust standard errors in parentheses

Table 9: Regression table - LH2 carrier and DES contract transportation cost

Bibliography

- Alanazi, K., Mittal, S., Hawkes, A., & Shah, N. (2025). Hydrogen and the decarbonization of the energy system in europe in 2050: A detailed model-based analysis. *International Journal of Hydrogen Energy*, *101*, 712–730. <https://doi.org/10.1016/j.ijhydene.2024.12.452>.
- Barner, L. (2024). A multi-commodity partial equilibrium model of imperfect competition in future global hydrogen markets. *Energy*, *311*. <https://doi.org/10.1016/j.energy.2024.133284>.
- Boissonnet, G., & Popiolek, N. (2024). Choix de la meilleure technologie pour le transport maritime d'hydrogène : Cas australie-japon à l'horizon 2050. *La Revue de l'Energie*, *2024/3 N°672*, 1230–1237. <https://doi.org/10.1016/j.ijhydene.2024.08.067>.
- Cayet, P., Azzaro-Pantel, C., Bourjade, S., & Muller-Vibes, C. (2024). Beyond the “bottom-up” and “top-down” controversy: A methodological inquiry into hybrid modeling methods for hydrogen supply chains. *International Journal of Production Economics*, *268*, 109091. <https://doi.org/10.1016/j.ijpe.2023.109091>.
- Chen, P. S.-L., Fan, H., & Abdussamie, N. (2025). Evaluation of hydrogen shipping cost for potential trade routes. *WMU Journal of Maritime Affairs*, *24*, 315–318. <https://doi.org/10.1007/s13437-025-00365-w>
- Chen, P. S.-L., Fan, H., Enshaei, H., Zhang, W., Shi, W., Abdussamie, N., Miwa, T., Qu, Z., & Yang, Z. (2023). A review on ports' readiness to facilitate international hydrogen trade. *International Journal of Hydrogen Energy*, *48*, 17351–17369. [//doi.org/10.1016/j.ijhydene.2023.01.220](https://doi.org/10.1016/j.ijhydene.2023.01.220)
- Daiyan, R., MacGill, I., & Khan, M. (2021). *Hysupply shipping tool v1.1*. UNSW. <https://www.globh2e.org.au/shipping-cost-tool>
- Diamantis, C., Ruby, A., Parmentier, P., & Goff, E. L. (2024). Optimal sizing of an ammonia production and transportation supply chain based on renewable electricity: Comparison between parametric study and a costs-emissions bi-objective optimization. *Renewable and Sustainable Energy Reviews*.
- Erdemir, D., & Dincer, I. (2024). A quicker route to hydrogen economy with ammonia. *International Journal of Hydrogen Energy*, *82*, 1230–1237. <https://doi.org/10.1016/j.ijhydene.2024.08.067>.

- Fattahi, A., Longa, F. D., & van der Zwaan, B. (2024). Opportunities of hydrogen and ammonia trade between Europe and MENA. *International Journal of Hydrogen Energy*, *83*, 967–974. <https://doi.org/10.1016/j.ijhydene.2024.08.021>
- Hampp, J., Duren, M., & Brown, T. (2023). Import options for chemical energy carriers from renewable sources to Germany. *PLoS ONE*, *18*(2):e0262340. <https://doi.org/10.1371/journal.pone.0281380>
- Hank, C., Holst, M., Thelen, C., Kost, C., Längle, S., Schaadt, A., & Smolinka, T. (2023). Power-to-x country analysis: Site-specific, comparative analysis for suitable power-to-x pathways and products in developing and emerging countries. *Fraunhofer Institute for Solar Energy Systems ISE*. https://india-re-navigator.com/public/uploads/1651644555-IRENA_Global_Trade_Hydrogen_2022.pdf
- International Energy Agency. (2024a). *Global hydrogen review 2024*. International Energy Agency. Paris. <https://www.iea.org/reports/global-hydrogen-review-2024>
- International Energy Agency. (2024b). *Global hydrogen review 2024*. International Energy Agency. Paris. <https://www.iea.org/reports/world-energy-investment-2024>
- International Energy Agency. (2024c). *World energy outlook 2024*. International Energy Agency. Paris. <https://www.iea.org/reports/world-energy-outlook-2024>
- IRENA. (2022). Global hydrogen trade to meet the 1.5°C climate goal: Part II – technology review of hydrogen carriers. *International Renewable Energy Agency*. https://india-re-navigator.com/public/uploads/1651644555-IRENA_Global_Trade_Hydrogen_2022.pdf
- Johnston, C., Khan, M. H. A., Amal, R., Daiyan, R., & MacGill, I. (2022). Shipping the sunshine: An open-source model for costing renewable hydrogen transport from Australia. *International Journal of Hydrogen Energy*, *47*, 20362–20377. <https://doi.org/10.1016/j.ijhydene.2022.04.156>
- Klaas, A.-K., Moritz, M., Wohlleben, D., & Sprenger, T. (2024). *Ewi global ptx cost tool documentation version 2.0*. Institute of Energy Economics at the University of Cologne gGmbH (EWI). <https://www.ewi.uni-koeln.de/en/tools/globales-ptx-produktions-und-importkostentool/>
- Lullo, G. D., Giwa, T., Okunlola, A., Davis, M., Mehedi, T., Oni, A., & Kumar, A. (2022). Large-scale long-distance land-based hydrogen transportation systems: A comparative techno-economic and greenhouse gas emission assessment (83). *International Journal of Hydrogen Energy*. <https://doi.org/10.1016/j.ijhydene.2022.08.131>
- Moritz, M., Schönfisch, M., & Schulte, S. (2023). Estimating global production and supply costs for green hydrogen and hydrogen-based green energy commodities. *International Journal of Hydrogen Energy*, *48*, 9139–9154. <https://doi.org/10.1016/j.ijhydene.2022.12.046>
- Núñez-Jimenez, A., & De-Blasio, N. (2022). “mighty: Model of international green hydrogen trade. *Belfer Center for Science and International Af-*

- fairs, Harvard Kennedy School.* <https://nrs.harvard.edu/URN-3:HUL.INSTREPOS:37373227>
- Osman, A. I., Nasr, M., Lichtfouse, E., Farghali, M., & Rooney, D. W. (2024). Hydrogen, ammonia and methanol for marine transportation. *Environmental Chemistry Letters*, *22*, 2151–2158. <https://doi.org/10.1007/s10311-024-01757-9>
- Perey, P., & Mulder, M. (2023). International competitiveness of low-carbon hydrogen supply to the northwest european market. *International Journal of Hydrogen Energy*, *48*, 1241–1254. <https://doi.org/10.1016/j.ijhydene.2022.10.011>
- Scheffler, F., Imdahl, C., Zellmer, S., & Herrmann, C. (2025). Techno-economic and environmental assessment of renewable hydrogen import routes from overseas in 2030. *Applied Energy*, *380*. <https://doi.org/10.1016/j.apenergy.2024.125073>
- Schuler, J., Ardone, A., & Fichtner, W. (2024). A review of shipping cost projections for hydrogen-based energy carriers. *International Journal of Hydrogen Energy*, *49*, 1497–1508. <https://doi.org/10.1016/j.ijhydene.2023.10.004>
- World port index 150. (2019). *Fraunhofer Institute for Solar Energy Systems ISE.* <https://msi.nga.mil/Publications/WPI>